AGU PUBLICATIONS

Water Resources Research

RESEARCH ARTICLE
10.1002/2015WR017225

A multivariate copula-based framework for dealing with hazard scenarios and failure probabilities

G. Salvadori[1], F. Durante[2], C. De Michele[3], M. Bernardi[4], and L. Petrella[5]

[1]Dipartimento di Matematica e Fisica, Università del Salento, Lecce, Italy, [2]Faculty of Economics and Management, Free University of Bozen-Bolzano, Bolzano, Italy, [3]Department of Hydraulic, Environmental, Roads and Surveying Engineering, Politecnico di Milano, Milano, Italy, [4]Department of Statistical Sciences, University of Padua, Padua, Italy, [5]Department of MEMOTEF, Sapienza University of Rome, Rome, Italy

Key Points:
- Methodological approach to multivariate risk assessment via copulas
- Probabilistically consistent definition of multivariate hazard scenario
- Calculation of the failure probability of different multivariate hazard scenarios

Correspondence to:
G. Salvadori,
gianfausto.salvadori@unisalento.it

Citation:
Salvadori, G., F. Durante, C. De Michele, M. Bernardi, and L. Petrella (2016), A multivariate copula-based framework for dealing with hazard scenarios and failure probabilities, *Water Resour. Res.*, *52*, 3701–3721, doi:10.1002/2015WR017225.

Received 12 MAR 2015
Accepted 21 APR 2016
Accepted article online 25 APR 2016
Published online 14 MAY 2016

Abstract This paper is of methodological nature, and deals with the foundations of Risk Assessment. Several international guidelines have recently recommended to select appropriate/relevant Hazard Scenarios in order to tame the consequences of (extreme) natural phenomena. In particular, the scenarios should be multivariate, i.e., they should take into account the fact that several variables, generally not independent, may be of interest. In this work, it is shown how a Hazard Scenario can be identified in terms of (i) a specific geometry and (ii) a suitable probability level. Several scenarios, as well as a Structural approach, are presented, and due comparisons are carried out. In addition, it is shown how the Hazard Scenario approach illustrated here is well suited to cope with the notion of Failure Probability, a tool traditionally used for design and risk assessment in engineering practice. All the results outlined throughout the work are based on the Copula Theory, which turns out to be a fundamental theoretical apparatus for doing multivariate risk assessment: formulas for the calculation of the probability of Hazard Scenarios in the general multidimensional case ($d \geq 2$) are derived, and worthy analytical relationships among the probabilities of occurrence of Hazard Scenarios are presented. In addition, the Extreme Value and Archimedean special cases are dealt with, relationships between dependence ordering and scenario levels are studied, and a counter-example concerning Tail Dependence is shown. Suitable indications for the practical application of the techniques outlined in the work are given, and two case studies illustrate the procedures discussed in the paper.

1. Introduction

Several international guidelines concerning the risk assessment in engineering practice are available in literature: see, among others, *European Committee for Standardization* [2002]; *ISO* [1998]; *JCSS* [2008]; *ISO* [2009a, 2009b]. An interesting novel approach is outlined in the Directive 2007/60/EC of The European Parliament and of The Council [*The European Parliament and The Council*, 2007]: it concerns the assessment and the management of flood risks, but the strategies proposed are paradigmatic, and can be adopted in all areas of environmental engineering (e.g., those concerning droughts, rainfall storms, sea storms, etc.). In particular, the cited Directive states that [*The European Parliament and The Council*, 2007, p. 30, chap. III, Article 6.3] the flood risk management should require the implementation of suitable "flood hazard maps covering the geographical areas which could be flooded according to the following scenarios: (a) floods with a low probability, or extreme event scenarios; (b) floods with a medium probability (likely return period $\geq$ 100 years); (c) floods with a high probability, where appropriate." Moreover, a multivariate approach is recommended [*The European Parliament and The Council*, 2007, p. 31, chap. III, Article 6.4], since it is suggested to consider, for each flood scenario, the following quantities: "(a) the flood extent; (b) water depths or water level, as appropriate; (c) where appropriate, the flow velocity or the relevant water flow." In turn, the scope of the Directive is twofold. On the one hand, the EU framework requires the specification of suitable stochastic models for flood events that are *per se* multivariate (viz., they involve a number of nonindependent variables for the characterization of a flood). On the other hand, relevant flood scenarios of interest are indicated, each associated with prescribed probability levels.

The EU guidelines pose nontrivial questions concerning the mathematical framework used to model natural threatening phenomena: in fact,

1. a notion of "(extreme) event scenario" must be introduced;
2. scenarios should be multivariate, viz. several variables, generally nonindependent, should be considered;
3. a suitable multivariate probability law must be specified.

Note that these issues are quite general, and are related to the (extreme) events associated with quite a few environmental phenomena (for a survey, see *Chebana* [2013] and *Straub* [2014]). In recent years, several investigations have focused on this troublesome matter. In literature [see e.g., *Reeve*, 2000, chap. 5; *Reeve et al*., 2004, chap. 7; *Kottegoda and Rosso*, 2008, chap. 9; *Liu et al*., 2015], the occurrence of environmental extreme event scenarios in a multivariate framework has been addressed trying to determine the probability corresponding to a failure region, considering failure modes with elements in series, in parallel, or mixed, both under independent and dependent circumstances. Specifically, in hydrology, examples are the joint occurrence of flood discharge at river confluences [*Raynal and Salas*, 1987; *Favre et al*., 2004; *Wang et al*., 2009; *Bender et al*., 2013], the superposition of river flooding and storm surges at coasts [*Kew et al*., 2013], or the important role of flood duration, besides peak discharge, for dike failure [*Vorogushyn et al*., 2010] and for flood losses [*Merz et al*., 2013]. Analogously, storm related coastal flooding events are mainly caused by high water levels, due to a combination of astronomical tide and storm surge, and high and long waves incident on the coast, through the effects of wave setup and runup—see *Masina et al*. [2015]. Moreover, several analyses highlighted relationships existing among the main oceanographic variables and proposed multivariate methods for the assessment of sea defenses—see e.g., *Hawkes* [2008]; *Hawkes et al*. [2002]; and *Ferreira and Soares* [2002]. Alternative methods that can deal with scenarios of arbitrary geometry can be found in *Girard and Stupfler* [2015]. In addition, recent advances concerning spatial risk assessment and quantification can be found in *Gräler* [2014], and references therein.

The target of this paper is to elaborate a probabilistically consistent framework that, according to various regulation requirements, is suitable for (*i*) dealing with the concept of multivariate hazard scenarios, and (*ii*) providing valuable tools for assessing the probability of threatening of (extreme) natural occurrences. Several are the elements of novelty introduced:

1. the concept of Hazard Scenario is defined at a general level via the notion of *Upper Set*, and is identified by (i) a specific geometry, and (ii) a suitable probability level;
2. general multidimensional formulas (for the case $d \geq 2$) are derived, both concerning the probabilities of occurrence of Hazard Scenarios and Failure Probabilities;
3. the formal connections between different Hazard Scenarios are investigated, and multivariate switching formulas for their respective probabilities are presented;
4. the Extreme Value and Archimedean special cases are dealt with, relationships between dependence ordering and scenario levels are studied, and a counter-example concerning Tail Dependence is shown.

Throughout the paper, several indications about the choice of the Hazard Scenario to be used in practical applications are given, and a Structural approach is dealt with as well.

The structure of this paper is as follows. Section 2 provides a general overview of the multivariate (copula-based) setting used in the paper. In section 3, the notion of Hazard Scenario is introduced, and several cases are discussed and compared; in addition, suitable indications concerning the application of the techniques outlined in the work are given. In section 4, the notion of Failure Probability is recalled, and it is shown how the Hazard Scenario approach illustrated here is well suited to cope with it. In section 5, two practical illustrations are shown. Finally, some conclusions are drawn in section 6.

2. The Theoretical Background

A convenient way to deal with multivariate phenomena, where the variables at play are generally nonindependent, is to use *Copulas* [*Nelsen*, 2006; *Salvadori et al*., 2007; *Durante and Sempi*, 2015]. Since the introduction of copulas in hydrology [*De Michele and Salvadori*, 2003], a number of papers in hydrology, as well as in other geophysical fields, have shown the theoretical and practical advantages of using a copula approach, and support their usage. For an overview concerning different ways of quantifying the risk of compound events see, among others, *Shiau* [2003]; *Salvadori* [2004]; *Gräler et al*. [2013]; *Salas and Obeysekera* [2014]; and *Serinaldi* [2015a]. A thorough list of relevant works is also available at the STAHY website (www.stahy.org). In particular, concerning selection/estimation/testing statistical procedures for copulas, the interested

reader may refer to *Genest and Favre* [2007]; *Genest et al*. [2009]; *Choroś et al*. [2010]; *Kojadinovic and Yan* [2010]; *Kojadinovic et al*. [2011]; *De Michele et al*. [2013]; *Fermanian* [2013]; *Joe* [2014]; *Salvadori et al*. [2014], and references therein. In addition, freeware for working with copulas, developed for the "R" package [*R Core Team*, 2013], is available online [*Hofert et al*., 2013; *Gräler*, 2015]. The results presented in the Case Studies (see section 5 below) have been obtained using the techniques outlined in the cited works, to which the reader is referred.

In the following, the same notation used in *Salvadori et al*. [2011, 2013] is adopted. In particular, $\mathbf{I}$ denotes the unit interval [0,1], and $\mathcal{L}_t$ indicates the level set at $t \in \mathbf{I}$ of the (joint) continuous distribution $\mathbf{F}(\mathbf{x})=\mathbf{C}(F_1(x_1),\ldots,F_d(x_d))$. Practically, $\mathcal{L}_t$ is the set of points in the d-dimensional Euclidean space $\mathbf{R}^d$ such that $\mathbf{F}(\mathbf{x})=t$—$\mathcal{L}_t$ will also be referred to as a "critical layer" of level t. Here $\mathbf{C}$ is the copula of the random vector $\mathbf{X}=(X_1,\ldots,X_d)$ describing the phenomenon under investigation, with univariate margins F_i's (assumed to be strictly increasing on their support), according to the representation given by *Sklar*'s Theorem [*Sklar*, 1959]. Similarly, $\overline{\mathcal{L}}_t$ denotes the critical layer of the (joint) survival function $\overline{\mathbf{F}}(\mathbf{x})=\mathbf{P}(X_1>x_1,\ldots,X_d>x_d)=\hat{\mathbf{C}}(\bar{F}_1(x_1),\ldots,\bar{F}_d(x_d))$, where $\hat{\mathbf{C}}$ is the survival copula of the X_i's, and $\bar{F}_i=1-F_i$ is the survival function of X_i, with $i=1,\ldots,d$. Note that $\hat{\mathbf{C}}$ can be written in terms of the copula $\mathbf{C}$ by using the Inclusion-Exclusion principle [see *Joe*, 2014, p. 27], since $\hat{\mathbf{C}}(\mathbf{u})=\overline{\mathbf{C}}(\mathbf{1}-\mathbf{u})$ for all $\mathbf{u} \in \mathbf{I}^d$, and $\overline{\mathbf{C}}$ is the survival function associated with $\mathbf{C}$ given by

$$\overline{\mathbf{C}}(\mathbf{u})=1-\sum_{i=1}^{d} u_i+\sum_{S\in\mathcal{P}} (-1)^{\#(S)}\mathbf{C}_S(u_i : i \in S), \tag{1}$$

where $\mathcal{P}$ is the set of all subsets of $\{1,2,\ldots,d\}$ with at least two elements, $\#(S)$ denotes the cardinality of S, and $\mathbf{C}_S(u_i : i \in S)$ represents the marginal copula of $\mathbf{C}$, with dimension equal to $\#(S)$, involving only those indices i's belonging to S. As will be made clear below, both $\mathcal{L}_t$ and $\overline{\mathcal{L}}_t$ play the role as of (critical) multivariate thresholds, with dimension $d-1$.

Furthermore, due to the assumption that the F_i's are strictly increasing, the Probability Integral Transform (hereinafter, *PIT*) viz., the relations

$$\mathbf{U}=(U_1,\ldots,U_d)=(F_1(X_1),\ldots,F_d(X_d))=\mathcal{T}_{\mathbf{F}}(\mathbf{X}), \tag{2}$$

and

$$\mathbf{X}=(X_1,\ldots,X_d)=(F_1^{-1}(U_1),\ldots,F_d^{-1}(U_d))=\mathcal{T}_{\mathbf{F}}^{-1}(\mathbf{U}), \tag{3}$$

are one-to-one. These formulas map the vector $\mathbf{U}$ living in $\mathbf{I}^d$ onto the vector $\mathbf{X}$ living in the d-dimensional Euclidean space $\mathbf{R}^d$ (and vice-versa)—see *Nelsen* [2006]; *Salvadori et al*. [2007]; and *Embrechts and Hofert* [2013]. Thanks to the invariance of copulas for strictly increasing transformations [*Nelsen*, 2006, Theorem 2.4.3], $\mathbf{U}$ and $\mathbf{X}$ share the same copula.

Note that, thanks to Sklar's Theorem, the PIT uniquely maps the probabilities of the events in $\mathbf{I}^d$ (as induced by the copula $\mathbf{C}$) onto $\mathbf{R}^d$ (as induced by $\mathbf{F}=\mathbf{C}(F_1,\ldots,F_d)$), and vice-versa; the same holds for $\hat{\mathbf{C}}$ and $\overline{\mathbf{F}}$. The role played by the univariate margins is only to geometrically remap such probabilities onto suitable regions in the Euclidean space $\mathbf{R}^d$ (and vice-versa), without affecting them. By the same token, also $\mathcal{L}_t$ and $\overline{\mathcal{L}}_t$ are mapped from $\mathbf{R}^d$ onto $\mathbf{I}^d$ (and vice-versa), thus becoming the level sets of $\mathbf{C}$ and $\hat{\mathbf{C}}$, respectively.

A further notion of interest is represented by the Kendall's function $\mathbf{K}$ [*Genest and Rivest*, 1993; *Barbe et al*., 1996; *Genest et al*., 2011] associated with the copula $\mathbf{C}$ of $\mathbf{X}$, which yields the following probability:

$$\mathbf{K}(t)=\mathbf{P}(\mathbf{F}(X_1,\ldots,X_d)\le t)=\mathbf{P}(\mathbf{C}(F_1(X_1),\ldots,F_d(X_d))\le t), \tag{4}$$

with $t \in \mathbf{I}$. For a graphical illustration of $\mathbf{K}$ see, e.g., in *Salvadori et al*. [2011, Figure 4].

Finally, analogously to the case of distribution functions, it is possible to define an *upper-orthant Kendall distribution function* $\hat{\mathbf{K}}$ associated with $\overline{\mathbf{F}}$, and given by

$$\hat{\mathbf{K}}(t)=\mathbf{P}\big(\overline{\mathbf{F}}(X_1,\ldots,X_d)\le t\big)=\mathbf{P}\big(\hat{\mathbf{C}}(\bar{F}_1(X_1),\ldots,\bar{F}_d(X_d))\le t\big), \tag{5}$$

with $t \in \mathbf{I}$. The survival function associated with $\hat{\mathbf{K}}$ will be (loosely) called *Survival Kendall*, and will be denoted by $\check{\mathbf{K}}$, viz. $\check{\mathbf{K}}=1-\hat{\mathbf{K}}$—for more details, see *Nappo and Spizzichino* [2009]; *Salvadori et al*. [2013, 2014]; and *Cousin and Di Bernardino* [2014]. For a graphical illustration of $\check{\mathbf{K}}$ see, e.g., in *Salvadori et al*. [2013, Figure 2].

3. Hazard Scenarios

In the following, the notion of Hazard Scenario will be fundamental. In particular, the concept of *Upper Set* [*Davey and Priestley*, 2002] will play an important role.

Definition 1 (Upper Set). $\mathcal{S} \subseteq \mathbf{R}^d$ is an Upper Set if, and only if, $\mathbf{x} \in \mathcal{S}$ and $\mathbf{y} \geq \mathbf{x}$ component-wise imply $\mathbf{y} \in \mathcal{S}$. ○

The notion of Upper Set well copes with the intuitive (and practical) reasoning that, if an occurrence is risky, then also "larger" realizations may be threatening. In turn, a possible definition of Hazard Scenario is as follows.

Definition 2 (Hazard Scenario). Let $\mathbf{X}$ be a random vector describing the phenomenon of interest. A Hazard Scenario (hereinafter, *HS*) of level $\alpha \in (0, 1)$ is any Upper Set $\mathcal{S}=\mathcal{S}_\alpha \subseteq \mathbf{R}^d$ such that the relation

$$\mathbf{P}(\mathbf{X} \in \mathcal{S})=\alpha \tag{6}$$

holds. ○

In order to keep the notation as simple as possible, in the following the dependence upon α will be suppressed whenever no confusion may arise. As a practical interpretation, a Hazard Scenario can be conceived as a set containing all the occurrences $\mathbf{x}$'s reputed to be "dangerous" (i.e., possibly affecting/damaging a given structure) according to some suitable criterion. In particular, if $\mathbf{x} \in \mathcal{S}$ and $\mathbf{y} \geq \mathbf{x}$ component-wise, then also $\mathbf{y}$ could be considered as a dangerous occurrence. Last, but not least, here it is important to stress the probabilistic foundational novelty brought by Definition 2 (viz., the α-level characterization of HS's), which is different from the traditional geometrical approach (as e.g., in *Serinaldi* [2015a, and references therein]). The advantages of the formalization of Hazard Scenarios proposed in this work will be well appreciated later, in the Case Studies section.

Since a Hazard Scenario is an Upper Set, it deals with situations where large values of the variables of interest are associated with dangerous conditions—as is common in many environmental engineering applications. When, on the contrary, small values of some variables X_i's may be dangerous (for instance, think of small discharges in case of droughts), formally it is enough to change the sign of the variables of interest, or carrying out other suitable transformations as in *AghaKouchak et al.* [2014].

As will be shown below, given a realization $\mathbf{x} \in \mathbf{R}^d$, there exist several ways to associate $\mathbf{x}$ with a suitable HS, occasionally denoted by $\mathcal{S}_\mathbf{x} \subseteq \mathbf{R}^d$ for the sake of clarity and notational convenience. Clearly, via the PIT (see equations (2) and (3)), there exists in $\mathbf{I}^d$ a unique realization $\mathbf{u}=\mathcal{T}_\mathbf{F}(\mathbf{x})$ corresponding to $\mathbf{x}$, as well as a unique region $\mathcal{S}_\mathbf{u} \subseteq \mathbf{I}^d$ corresponding to $\mathcal{S}_\mathbf{x}$. In turn, the knowledge of the copula at play may suffice to calculate the level of $\mathcal{S}_\mathbf{u}$, and hence of $\mathcal{S}_\mathbf{x}$.

In literature, several scenarios are usually considered. The choice of a specific HS to be used in practice may depend upon two different, and complementary, criteria: viz., the type of events considered to be menacing, and their probabilities of occurrence, as will be made clear below (see also Table 1, the examples presented later in section 3.1, and the survey in *Serinaldi* [2015a]).

1. **"OR" scenario** $\mathcal{S}^\vee$. A d-dimensional OR HS is given by the region

$$\mathcal{S}^\vee_\mathbf{x}=\bigcup_{i=1}^{d}(\mathbf{R}\times\cdots\times(x_i,+\infty)\times\cdots\times\mathbf{R}), \tag{7}$$

and the associated level α is

$$\alpha^\vee_\mathbf{x}=\mathbf{P}\left(\mathbf{X} \in \mathcal{S}^\vee_\mathbf{x}\right)=1-\mathbf{C}(F_1(x_1),\ldots,F_d(x_d)). \tag{8}$$

For the realization of the event $\{\mathbf{X} \in \mathcal{S}^\vee_\mathbf{x}\}$ it is sufficient that one of the variables X_i's, with $i=1,\ldots,d$, exceeds the corresponding threshold x_i. The shape of a bivariate OR HS is illustrated in Figure 1a, considering the pair $(U, V) \in \mathbf{I}^2$ (see, among others, *Yue and Rasmussen* [2002]; *Shiau* [2003], and also *Salvadori* [2004]; *Salvadori and De Michele* [2004]; *De Michele et al.* [2005]).

Table 1. Literature Survey (in a Chronological Order) Concerning the Usage of the Approaches OR, AND, Kendall (K.), and Survival Kendall (S.K.)—See Text[a]

Reference	OR	AND	K.	S.K.
Yue [2000a]	*			
Yue [2000b]	*			
Yue [2001a]	*			
Yue [2001b]	*			
Yue [2002]	*			
Yue and Rasmussen [2002]	*	*		
Yue and Wang [2004]	*			
Shiau [2003]	*	*		
Salvadori and De Michele [2004]	*	*	*	
De Michele et al. [2005]	*	*	*	
Shiau [2006]	*	*		
Salvadori and De Michele [2007]	*	*	*	
Salvadori et al. [2007]	*	*	*	
Poulin et al. [2007]		*		
Shiau and Modarres [2009]				
Karmakar and Simonovic [2009]	*			
Salvadori and De Michele [2010]	*	*	*	
Salvadori et al. [2011]	*	*	*	
Klein et al. [2011]	*	*	*	
Fan et al. [2012]		*		
Zhang and Singh [2012]		*		
Corbella and Stretch [2012]			*	
Salvadori et al. [2013]			*	*
De Michele et al. [2013]				*
Li et al. [2013b]	*			
Li et al. [2013a]	*	*		
Lian et al. [2013]	*	*		
Gräler et al. [2013]	*	*	*	
Chen et al. [2013]	*	*	*	
Zhang et al. [2013]	*	*	*	
Requena et al. [2013]	*	*	*	
Salvadori et al. [2014]				*
Jeong et al. [2014]	*	*		
Serinaldi [2015a]	*	*	*	
Mitkova and Halmova [2014]	*	*		
AghaKouchak [2014]	*			
AghaKouchak et al. [2014]				*
Xu et al. [2014]	*			
Volpi and Fiori [2014]	*		*	
Salvadori et al. [2015]				*
Ming et al. [2015]		*		
Liu et al. [2015]		*		
Serinaldi [2015b]	*	*	*	*

[a]The "*" indicates which approach is discussed in the corresponding reference.

2. **"AND" scenario** $\mathcal{S}^{\wedge}$. A d-dimensional AND HS is given by the region

$$\mathcal{S}^{\wedge}_{\mathbf{x}} = \bigcap_{i=1}^{d} (\mathbf{R} \times \cdots \times (x_i, +\infty) \times \cdots \times \mathbf{R}), \tag{9}$$

and the associated level α is

$$\alpha^{\wedge}_{\mathbf{x}} = \mathbf{P}\left(\mathbf{X} \in \mathcal{S}^{\wedge}_{\mathbf{x}}\right) = \hat{\mathbf{C}}(\bar{F}_1(x_1), \ldots, \bar{F}_d(x_d)). \tag{10}$$

For the realization of the event $\{\mathbf{X} \in \mathcal{S}^{\wedge}_{\mathbf{x}}\}$ it is necessary that all the variables X_i's, with $i = 1, \ldots, d$, exceed the corresponding thresholds x_i's. The shape of a bivariate AND HS $\mathcal{S}^{\wedge}_{u,v}$ is illustrated in Figure 1b, considering the pair $(U, V) \in \mathbf{I}^2$ (see, among others, *Yue and Rasmussen* [2002]; *Shiau* [2003], and also *Salvadori* [2004]; *Salvadori and De Michele* [2004]; *De Michele et al.* [2005]).

3. "Kendall" scenario $\mathcal{S}^{\mathbf{K}}$. Let $\mathbf{x} \in \mathbf{R}^d$ be a given occurrence, with $t = \mathbf{F}(\mathbf{x})$, and let $\mathcal{L}_t$ be the level set crossing $\mathbf{x}$. A d-dimensional Kendall HS is given by the region

$$\mathcal{S}^{\mathbf{K}}_t = \{\mathbf{y} \in \mathbf{R}^d : \mathbf{F}(\mathbf{y}) > t\} = \{\mathbf{y} \in \mathbf{R}^d : \mathbf{C}(F_1(y_1), \ldots, F_d(y_d)) > t\}, \tag{11}$$

and the associated level α is [*Salvadori et al.*, 2011]

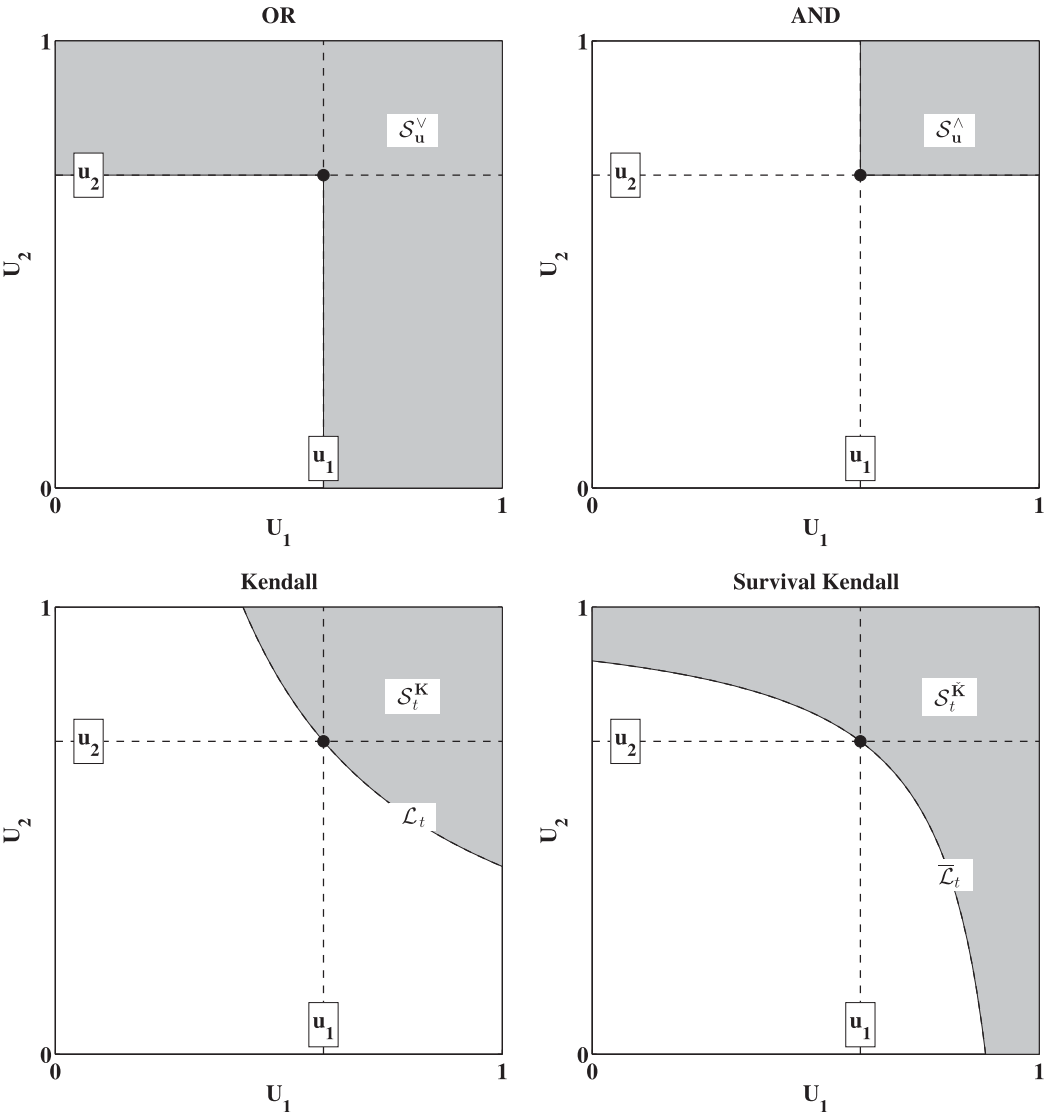

Figure 1. Bivariate illustration of the Hazard Scenarios investigated here (*shaded* areas) according to different approaches, in the copula domain—see text: respectively, the (top-left) OR, (top-right) AND, (bottom-left) Kendall, and (bottom-right) the Survival Kendall. In the Kendall case, the lower bound of the hazard region corresponds to the critical isoline $\mathcal{L}_t$, while in the Survival Kendall case it corresponds to $\overline{\mathcal{L}}_t$—see text.

$$\alpha_{\mathbf{u}}^{\mathbf{K}}=\alpha_{\mathbf{x}}^{\mathbf{K}}=\alpha_t^{\mathbf{K}}=\mathbf{P}\left(\mathbf{X}\in\mathcal{S}_t^{\mathbf{K}}\right)=1-\mathbf{K}(t), \tag{12}$$

where $t=\mathbf{C}(\mathbf{u})=\mathbf{F}(\mathbf{x})$. A bivariate Kendall HS is illustrated in Figure 1c, considering the pair $(U,V)\in\mathbf{I}^2$. Roughly speaking, $\mathcal{S}_t^{\mathbf{K}}$ is the region "exceeding" the critical layer $\mathcal{L}_t$: it is in this very sense that $\mathcal{L}_t$ may represent a critical multivariate threshold.

4. **"Survival Kendall" scenario** $\mathcal{S}^{\check{\mathbf{K}}}$. Let $\mathbf{x}\in\mathbf{R}^d$ be a given occurrence, with $t=\overline{\mathbf{F}}(\mathbf{x})$, and let $\overline{\mathcal{L}}_t$ be the survival level set crossing $\mathbf{x}$. A d-dimensional Survival Kendall HS is given by the region

$$\mathcal{S}_t^{\check{\mathbf{K}}}=\{\mathbf{y}\in\mathbf{R}^d:\overline{\mathbf{F}}(\mathbf{y})<t\}=\{\mathbf{y}\in\mathbf{R}^d:\hat{\mathbf{C}}(\bar{F}_1(y_1),\ldots,\bar{F}_d(y_d))<t\}, \tag{13}$$

and the associated level α is [*Salvadori et al.*, 2013, 2014]

$$\alpha_{\mathbf{u}}^{\check{\mathbf{K}}}=\alpha_{\mathbf{x}}^{\check{\mathbf{K}}}=\alpha_t^{\check{\mathbf{K}}}=\mathbf{P}\left(\mathbf{X}\in\mathcal{S}_t^{\check{\mathbf{K}}}\right)=1-\check{\mathbf{K}}(t)=\hat{\mathbf{K}}(t), \tag{14}$$

where $t=\hat{\mathbf{C}}(\mathbf{1}-\mathbf{u})=\overline{\mathbf{F}}(\mathbf{x})$. A bivariate Survival Kendall HS is illustrated in Figure 1d, considering the pair $(U,V)\in\mathbf{I}^2$. Roughly speaking, $\mathcal{S}_t^{\check{\mathbf{K}}}$ is the region "exceeding" the survival critical layer $\overline{\mathcal{L}}_t$: it is in this very sense that $\overline{\mathcal{L}}_t$ may represent a critical multivariate threshold.

5. **"Structural" scenario** $\mathcal{S}^{\Psi}$. As a further interesting point, it is worth noting that the notion of Hazard Scenario introduced here is also well suited for dealing with a *structural approach* to the risk assessment, as outlined, e.g., in *De Michele et al*. [2005]; *Requena et al*. [2013]; *Volpi and Fiori* [2014]; and *Salvadori et al*. [2015] [see also *Kottegoda and Rosso*, 2008, sec. 9.1.4]. In this case, the set of dangerous occurrences (as well as its shape) is dictated by a *structure function* Ψ accounting for the interactions between the physical structure and the loads acting on it.

   Generally speaking, for a suitable critical threshold $z \in \mathbf{R}$, a structural HS can be defined as

$$\mathcal{S}_z^{\Psi} = \{\mathbf{x} \in \mathbf{R}^d : \Psi(\mathbf{x}) > z\}, \tag{15}$$

   where $\Psi : \mathbf{R}^d \to \mathbf{R}$, and the only requirements are that (*i*) Ψ be continuous, and (*ii*) $\mathbf{y} \geq \mathbf{x}$ componentwise imply $\Psi(\mathbf{y}) \geq \Psi(\mathbf{x})$. The probabilistic characterization of a structural HS $\mathcal{S}_z^{\Psi}$ is provided by the associated level α given by

$$\alpha_z^{\Psi} = \mathbf{P}\left(\mathbf{X} \in \mathcal{S}_z^{\Psi}\right) = \mathbf{P}(\Psi(\mathbf{X}) > z), \tag{16}$$

   whose computation, however, may turn out to be an awkward task from an analytical point of view, especially when Ψ is a (highly) nonlinear function—as, e.g., in the illustration presented in section 5.2). Should this be the case, a viable solution is to resort to a Monte Carlo approach [see *Straub*, 2014, and references therein]. Practically, a huge sample of occurrences $\mathbf{x}$'s (say, of size $M \gg 1$), extracted from the distribution describing the phenomenon, is first simulated. Then, α_z^{Ψ} can be empirically estimated as the percentage of realizations such that $\Psi(\mathbf{x}) > z$. An uncertainty analysis can be carried out as illustrated in section 5.

The shapes of the four Hazard Scenarios OR, AND, Kendall, and Survival Kendall introduced above are ruled by, respectively, equations (7), (9), (11), and (13), while the corresponding probabilities are tuned by, respectively, equations (8), (10), (12), and (14). On the one hand, the dangerousness of a set of occurrences can be "qualified" via the specific geometry of a HS; on the other hand, the level of a HS may "quantify" the threatening of the same set.

The plots shown in Figure 1, together with the monotonic property of probability measures (viz., if $A \subseteq B$ then $\mathbf{P}(A) \leq \mathbf{P}(B)$) yield the following results. Note that, in general, for a given $t \in \mathbf{I}$, $\mathcal{S}_t^{\mathbf{K}}$ and $\mathcal{S}_t^{\check{\mathbf{K}}}$ may overlap over a set having positive probability, i.e., $\mathbf{P}\left(\mathbf{X} \in \mathcal{S}_t^{\mathbf{K}} \cap \mathcal{S}_t^{\check{\mathbf{K}}}\right) > 0$: for this reason, the Kendall and the Survival Kendall cases will be dealt with separately.

1. **The Kendall case.** Let $\mathbf{u} = \mathbf{F}(x_1, \ldots, x_d) \in \mathbf{I}^d$ be fixed, and let $\mathcal{L}_t$ be the critical layer crossing $\mathbf{u}$, where $t = \mathbf{C}(\mathbf{u})$. Evidently,

$$\mathcal{S}_{\mathbf{u}}^{\wedge} \subseteq \mathcal{S}_t^{\mathbf{K}} \subseteq \mathcal{S}_{\mathbf{u}}^{\vee}, \tag{17}$$

   and hence

$$\alpha_{\mathbf{u}}^{\wedge} \leq \alpha_t^{\mathbf{K}} \leq \alpha_{\mathbf{u}}^{\vee}. \tag{18}$$

   Thanks to equation (8), $\alpha_{\mathbf{u}}^{\vee}$ is constant as $\mathbf{u}$ runs over $\mathcal{L}_t$, as well as $\alpha_t^{\mathbf{K}}$ (thanks to equation (12)), whereas $\alpha_{\mathbf{u}}^{\wedge}$ generally changes. However, while $\mathcal{S}_t^{\mathbf{K}}$ is unique for all occurrences belonging to $\mathcal{L}_t$, the HS $\mathcal{S}_{\mathbf{u}}^{\vee}$'s reshape and partially overlap.
2. **The Survival Kendall case.** Let $\mathbf{u} = \overline{\mathbf{F}}(x_1, \ldots, x_d) \in \mathbf{I}^d$ be fixed, and let $\overline{\mathcal{L}}_t$ be the survival critical layer crossing $\mathbf{u}$, where $t = \hat{\mathbf{C}}(\mathbf{1} - \mathbf{u})$. Evidently,

$$\mathcal{S}_{\mathbf{u}}^{\wedge} \subseteq \mathcal{S}_t^{\check{\mathbf{K}}} \subseteq \mathcal{S}_{\mathbf{u}}^{\vee}, \tag{19}$$

   and hence

$$\alpha_{\mathbf{u}}^{\wedge} \leq \alpha_t^{\check{\mathbf{K}}} \leq \alpha_{\mathbf{u}}^{\vee}. \tag{20}$$

   Thanks to equation (10), $\alpha_{\mathbf{u}}^{\wedge}$ is constant as $\mathbf{u}$ runs over $\overline{\mathcal{L}}_t$, as well as $\alpha_t^{\check{\mathbf{K}}}$ (thanks to equation (14)), whereas $\alpha_{\mathbf{u}}^{\vee}$ generally changes. However, while $\mathcal{S}_t^{\check{\mathbf{K}}}$ is unique for all occurrences belonging to $\overline{\mathcal{L}}_t$, the HS $\mathcal{S}_{\mathbf{u}}^{\wedge}$'s reshape and partially overlap.

3.1. Practical Usage of Hazard Scenarios

As stressed in *Serinaldi* [2015a], the use of a specific HS should only be ruled by (*i*) suitable physical considerations about the phenomenon under consideration, and (*ii*) specific combinations of the most relevant

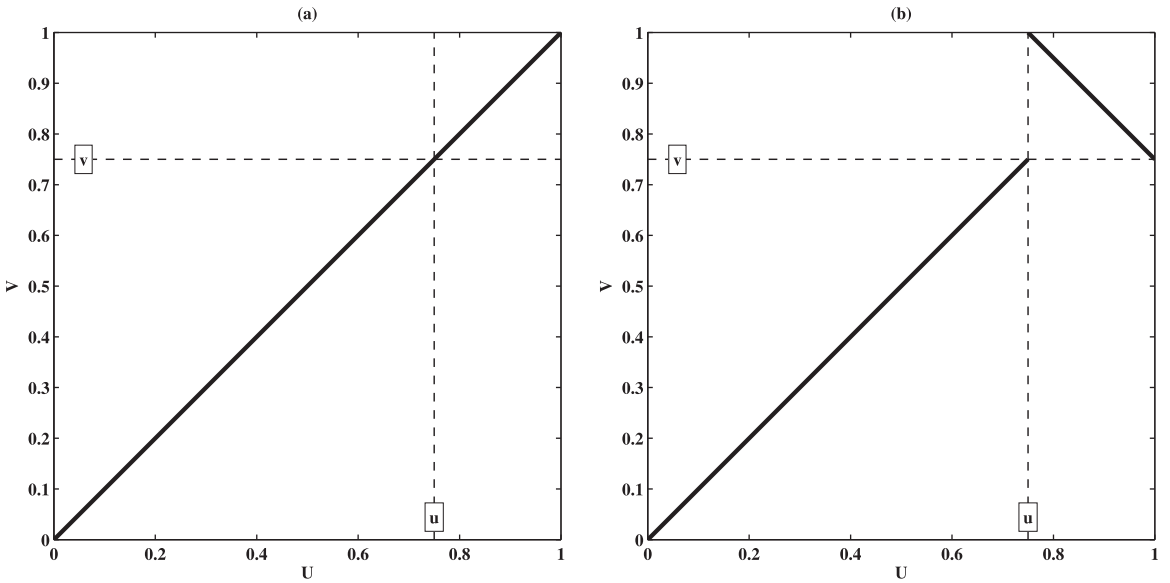

Figure 2. Support of the 2-copulas mentioned in the text: here $u=v=t=3/4$. (a) The comonotone 2-copula $\mathbf{C}_1=\mathbf{M}_2$. (b) The 2-copula $\mathbf{C}_2$.

variables that give rise to the occurrence of dangerous events. In this section, several practical examples are presented: the intention is to provide indications useful to select a proper HS suitable for dealing with the problem under investigation. Once the shape of a scenario has been decided (e.g., by choosing one of the alternatives mentioned above—see also sections 4 and 5), then it is only the corresponding probability (viz., the level α) that tunes the degree of threatening.

Mimicking [*Shiau*, 2003, p. 56], the following sentence well depicts the issue: the use of OR or AND HS's "depends on what situations will destroy the structure. Under the condition that either flood peak or flood volume exceeding a certain magnitude will cause damage, then [the OR approach can be used]. On the other hand, when the flood volume and flood peak must exceed a certain magnitude that will cause damage, then [the AND approach is used]." Further examples are given below; in addition, Table 1 provides a short list of some relevant works present in literature using the approaches mentioned throughout the paper.

3.1.1. "OR" Scenario $\mathcal{S}^{\vee}$

An example concerning the use of the OR scenario concerns the evaluation of dangerous flood events at the confluence of two rivers, where the threatening occurrence can be due to the contribution of one river, or the other, or both [see e.g., *Favre et al*., 2004; *Wang et al*., 2009; *Bender et al*., 2013]. Further hydrological examples concerning the usage of the OR approach can be found in section 5.1, and in the references cited in Table 1 (column "OR").

3.1.2. "AND" Scenario $\mathcal{S}^{\wedge}$

A recent example concerning the use of the AND approach is provided by *Dung et al*. [2015], involving flood events. In this work it is argued that the Mekong Delta (Vietnam) is at risk if both flood peak and flood volume are large. In fact, since socio-economic and agricultural activities are well trained to withstand floods, large discharge values exceeding dike levels do not automatically imply a disaster. For a flood event to become a menace, also a large volume is needed. For instance, the 2000's event, when extremely large volumes were combined with large peak discharges, represents a significant example, which caused the most disastrous flood in recent years. Further hydrological examples concerning the usage of the AND approach can be found in the references cited in Table 1 (column "AND").

While the OR and AND paradigms mentioned above are somewhat intuitive and common in multivariate hydrological practice (see, e.g., many of the references given in this work), the approaches *à la Kendall* entail a change of perspective. In fact, both the OR and the AND cases are determined by a given occurrence $\mathbf{x}$, as implied by equations (7) and (9), respectively. Instead, both the Kendall and the Survival Kendall HS's are identified via a critical layer of level t, viz. an infinity of occurrences $\mathbf{x}$'s. More precisely, it is easily seen that (for the OR case)

$$\mathcal{S}_t^{\mathbf{K}} = \bigcap_{\mathbf{u}\in\mathcal{L}_t} \mathcal{S}_{\mathbf{u}}^{\vee}, \tag{21}$$

as shown in Figure 1c, and (for the AND case)

$$\mathcal{S}_t^{\check{\mathbf{K}}} = \bigcup_{\mathbf{u}\in\mathcal{L}_t} \mathcal{S}_{\mathbf{u}}^{\wedge}, \tag{22}$$

as shown in Figure 1d. Thus, the Kendall and the Survival Kendall HS's represent, respectively, the intersection and the union of infinite OR and AND Hazard Scenarios, and can be (uniquely) associated with any of the occurrences **x**'s lying over the corresponding critical layer of level *t* identifying the dangerous region. Roughly speaking, $\mathcal{S}_t^{\mathbf{K}}$ and $\mathcal{S}_t^{\check{\mathbf{K}}}$ "summarize" all the threatening realizations characterizing the OR and AND cases for a given level *t*. This latter feature emphasizes the probabilistic nature of the approaches *à la Kendall*: the dangerous regions are identified via a strategy that takes into account the distribution function of **X** and its level curves. Instead, in the OR and AND cases, the shapes of the hazard regions are determined *a priori*. In turn, intrinsically, the Kendall and the Survival Kendall HS's do not have a direct interpretation, say, in physical/structural terms (only the pure stochastic component is considered): viz., they do not identify a priori which variables may represent the main sources of risk. Thus, the procedures *à la Kendall* should typically be used for carrying out a *preliminary risk assessment* survey, independently of the structure under consideration, in order to puzzle out what is likely to be expected at a given site in terms of probabilities of (multivariate) occurrences.

3.1.3. "Kendall" Scenario $\mathcal{S}^{\mathbf{K}}$

An analysis of pros and cons of the Kendall approach can be found in *Corbella and Stretch* [2012], involving a coastal engineering case study. In this work concerning coastal erosion, it is argued that the erosion risk (viz., the structural risk) is often associated with numerous combinations of sea storm characteristics: these latter, despite having the same multivariate probability, may cause very different erosion outcomes. The paper shows that a preliminary analysis via a Kendall approach turns out to be very useful, since the multivariate Kendall return periods for wave height and duration have the highest correlation with the erosion return periods, i.e., they well represent the structural risk. Further hydrological examples concerning the usage of the Kendall approach can be found in the references cited in Table 1 (column "Kendall").

3.1.4. "Survival Kendall" Scenario $\mathcal{S}^{\check{\mathbf{K}}}$

The Survival Kendall approach has been introduced in *Salvadori et al*. [2013] as a dual counterpart of the Kendall one. As compared to this latter modus operandi, it defines regions of "safe" events that are bounded, thus guaranteeing that nondangerous occurrences take on bounded values of all variables. The Survival Kendall approach has been applied, for instance, in *AghaKouchak et al*. [2014] for the analysis of the 2014 California drought. Here the compound event given by the combination of extreme precipitation and temperature conditions observed in 2014 in California appears to be a 200 year extreme event. Instead, the univariate risk estimation approaches, commonly used in practice, significantly underestimate or overestimate the return period (viz., the risk of occurrence) of the drought. Further hydrological examples concerning the usage of the Survival Kendall approach can be found in the references cited in Table 1 (column "Survival Kendall").

3.2. Relationships Between HS's Probabilities

The formulas shown above can be combined in order to express a given scenario level as a function of the probabilities of other scenarios. For the ease of illustration, only the bivariate case will be presented here: general switching formulas for the *d*-dimensional case, with $d \geq 2$, can be found in Appendix A. According to equations (8) and (10),

$$\begin{aligned} \alpha_{u_1,u_2}^{\vee} &= 1-\mathbf{C}(u_1,u_2) \\ &= 1-\left[u_1+u_2-1+\hat{\mathbf{C}}(1-u_1,1-u_2)\right] \\ &= 2-\left(u_1+u_2+\alpha_{u_1,u_2}^{\wedge}\right). \end{aligned} \tag{23}$$

Similarly, via equations (12) and (14),

$$\begin{aligned}\alpha^{\mathbf{K}}_{u_1,u_2} &= 1-\mathbf{K}(t)\\ &= 1-\mathbf{K}(\mathbf{C}(u_1,u_2))\\ &= 1-\mathbf{K}(u_1+u_2-1+\alpha^{\wedge}_{u_1,u_2}),\end{aligned} \tag{24}$$

and

$$\begin{aligned}\alpha^{\check{\mathbf{K}}}_{u_1,u_2} &= 1-\check{\mathbf{K}}(t)\\ &= 1-\check{\mathbf{K}}(\hat{\mathbf{C}}(1-u_1,1-u_2))\\ &= 1-\check{\mathbf{K}}(\alpha^{\wedge}_{u_1,u_2}).\end{aligned} \tag{25}$$

In turn, any probability can be rewritten in terms of $\alpha^{\wedge}_{\mathbf{u}}$ and, conversely, $\alpha^{\wedge}_{\mathbf{u}}$ can be computed as a function of the other scenarios' probabilities. It is worth stressing that the formulas given above show how the probabilities of occurrence of different HS are analytically linked: thus, any further numerical comparison in a specific case study may be superfluous.

3.3. HS and Dependence Ordering

In literature, several ways of "ordering" copulas are present: for an overview, among others see *Nelsen* [2006, chap. 5], *Salvadori et al*. [2007, Appendix B], and *Joe* [2014, chap. 2], and references therein. Now let $\mathbf{u} \in \mathbf{I}^d$ (or, equivalently, $\mathbf{x} \in \mathbf{R}^d$) be fixed, and consider two different copulas $\mathbf{C}_1$ and $\mathbf{C}_2$, which generate the distributions $\mathbf{F}_1=\mathbf{C}_1(F_1,\ldots,F_d)$ and $\mathbf{F}_2=\mathbf{C}_2(F_1,\ldots,F_d)$, with the same margins F_i's. An interesting question concerns how the level of a HS may change as $\mathbf{C}_2$ is substituted for $\mathbf{C}_1$, under specific conditions concerning the order relation between $\mathbf{C}_1$ and $\mathbf{C}_2$. Below, several cases will be investigated.

Suppose that $\mathbf{C}_1 \preceq \mathbf{C}_2$ in the "POD" order [*Nelsen*, 2006, Def. 5.7.2], viz.

$$\mathbf{C}_1(\mathbf{u}) \le \mathbf{C}_2(\mathbf{u}) \quad \text{and} \quad \hat{\mathbf{C}}_1(\mathbf{1}-\mathbf{u}) \le \hat{\mathbf{C}}_2(\mathbf{1}-\mathbf{u}) \tag{26}$$

for all $\mathbf{u} \in \mathbf{I}^d$. In turn, since $1-\mathbf{C}_1(\mathbf{u}) \ge 1-\mathbf{C}_2(\mathbf{u})$, then

$$\alpha^{\vee}_{\mathbf{u}}(\mathbf{C}_1) \ge \alpha^{\vee}_{\mathbf{u}}(\mathbf{C}_2) \tag{27}$$

according to equation (8), and

$$\alpha^{\wedge}_{\mathbf{u}}(\mathbf{C}_1) \le \alpha^{\wedge}_{\mathbf{u}}(\mathbf{C}_2) \tag{28}$$

according to equation (10). As a consequence, for given $\mathbf{u} \in \mathbf{I}^d$ (or, equivalently, $\mathbf{x} \in \mathbf{R}^d$), $\alpha^{\vee}_{\mathbf{u}}(\mathbf{C})$ decreases as $\mathbf{C}$ increases in the POD order, whereas, on the contrary, $\alpha^{\wedge}_{\mathbf{u}}(\mathbf{C})$ increases in the same direction as of the POD order, and takes on its maximum for the comonotone copula $\mathbf{M}_d(\mathbf{u})=\min\{u_1,\ldots,u_d\}$, viz. the Fréchet upper-bound. Now, in the bivariate case, consider the occurrence (x, y), and the corresponding HS's $\mathcal{S}^{\vee}_{x,y}$ and $\mathcal{S}^{\wedge}_{x,y}$. Then, under the OR approach, $\mathbf{P}(\mathbf{X} \in \mathcal{S}^{\vee}_{x,y})$ gets smaller as the dependence increases, and thus $\mathcal{S}^{\vee}_{x,y}$ is less and less likely to happen. Instead, under the AND approach, $\mathbf{P}(\mathbf{X} \in \mathcal{S}^{\wedge}_{x,y})$ gets larger as the dependence increases, and thus $\mathcal{S}^{\wedge}_{x,y}$ is more and more likely to happen. A rough conclusion is as follows: an increase of the dependence may not necessarily entail a growth of the risk, since the latter may also depend upon the HS at play.

Concerning the approaches *à la Kendall*, involving either the copula $\mathbf{C}$ or the survival copula $\hat{\mathbf{C}}$, comparisons in the POD order may not always be meaningful: in this case, the copula rules both the probabilities and the geometry of the HS. In fact, let $\mathbf{u} \in \mathbf{I}^d$, and set $t_1=\mathbf{C}_1(\mathbf{u})$ and $t_2=\mathbf{C}_2(\mathbf{u})$. In general, it will be $t_1 \neq t_2$, and the two critical layers $\mathcal{L}^{\mathbf{C}_1}_{t_1}$ (associated with $\mathbf{C}_1$) and $\mathcal{L}^{\mathbf{C}_2}_{t_2}$ (associated with $\mathbf{C}_2$), both crossing $\mathbf{u}$, will be geometrically different, as well as the geometry of the corresponding HS's $\mathcal{S}^{\mathbf{K}(\mathbf{C}_1)}_{t_1}$ and $\mathcal{S}^{\mathbf{K}(\mathbf{C}_2)}_{t_2}$: in particular, these two HS's may partially overlap. The same situation is present in the survival case. In turn, thanks to equations (12) and (14), the following relations can be stated:

$$\alpha^{\mathbf{K}}_{\mathbf{u}}(\mathbf{C}_1) \le \alpha^{\mathbf{K}}_{\mathbf{u}}(\mathbf{C}_2) \iff \mathbf{K}_{\mathbf{C}_2}(t_2) \le \mathbf{K}_{\mathbf{C}_1}(t_1), \tag{29}$$

and

$$\alpha^{\check{\mathbf{K}}}_{\mathbf{u}}(\hat{\mathbf{C}}_1) \le \alpha^{\check{\mathbf{K}}}_{\mathbf{u}}(\hat{\mathbf{C}}_2) \iff \check{\mathbf{K}}_{\hat{\mathbf{C}}_2}(t_2) \le \check{\mathbf{K}}_{\hat{\mathbf{C}}_1}(t_1). \tag{30}$$

Note that, in general, [*Capéraà et al*., 1997; *Nelsen et al*., 2003], the ordering among Kendall functions does not imply (and neither it is implied) by the POD ordering among the respective copulas.

A special situation concerns the case of the bivariate Extreme Value (hereinafter, *EV)* copulas [*Beirlant et al*., 2004], for which the analytical expression of the Kendall function is known [*Ghoudi et al*., 1998], and is given by

$$\mathbf{K}(t)=t-(1-\tau_{\mathbf{C}})\,t\ln t, \tag{31}$$

where $\tau_{\mathbf{C}}$ is the value of the Kendall τ associated with the 2-copula $\mathbf{C}$ [*Nelsen*, 2006; *Salvadori et al*., 2007]. Clearly, EV 2-copulas with the same τ share the same function $\mathbf{K}$. In turn—see equation (12),

$$\tau_{\mathbf{C}_1}\le\tau_{\mathbf{C}_2}\quad\Longleftrightarrow\quad\mathbf{K}_{\mathbf{C}_1}(t)\le\mathbf{K}_{\mathbf{C}_2}(t)\quad\Longleftrightarrow\quad\alpha^{\mathbf{K}}_{\mathbf{u}}(\mathbf{C}_1)\ge\alpha^{\mathbf{K}}_{\mathbf{u}}(\mathbf{C}_2). \tag{32}$$

Thus, in the bivariate EV case, the probability of occurrence of $\mathcal{S}^{\mathbf{K}}_{\mathbf{u}}$ gets smaller as the dependence increases, and thus $\mathcal{S}^{\mathbf{K}}_{\mathbf{u}}$ is less likely to happen. To the best of our knowledge, no generalizations of equation (31) to dimensions $d>2$ are presently known.

A specific ordering can be introduced also for Archimedean copulas [*Nelsen*, 2006, Theorem 4.4.2], provided that suitable subadditivity conditions are satisfied by appropriate compositions of the generators and their inverses. However, due to the presence of awkward technical issues, the topic is outside the scope of this paper.

A further interesting point concerns the notion of Upper Tail Dependence Coefficient [see *Nelsen*, 2006, sec. 5.4; *Salvadori et al*., 2007, sec. 3.4 and 5.3], frequently considered in applications for dealing with the extreme joint behavior of the variables at play [see e.g., *Poulin et al*., 2007; *AghaKouchak et al*., 2013; *Serinaldi*, 2013, and references therein].

Here the question is as follows (involving the bivariate case): how much does the level of a HS change as the upper tail dependence coefficient $\lambda_{\uparrow}=\lim_{t\to1^-}\mathbf{P}(U>t|V>t)$ changes (here, $(U,V)\sim\mathbf{C}$)? Unfortunately, no general answer is possible, as the following bivariate counter-example shows. Let $t\in\mathbf{I}$ be fixed, and let $\mathbf{C}_1(u,v)=\mathbf{M}_2(u,v)=\min\{u,v\}$ be the comonotone 2-copula, and let $\mathbf{C}_2$ be the 2-copula whose support is depicted in Figure 2b. Evidently, $\lambda_{\uparrow}(\mathbf{M}_2)=1\neq0=\lambda_{\uparrow}(\mathbf{C}_2)$. However, $\alpha^{\wedge}_{t,t}(\mathbf{M}_2)=1-t=\alpha^{\wedge}_{t,t}(\mathbf{C}_2)$, viz. the levels do not change. In simple words, apparently the AND approach does not take into account possible changes of the dependence structure "above" the pair (t,t).

Here it is worth stressing that the Upper Tail Dependence Coefficient is related to the asymptotic tail behavior, whereas the probability of occurrence of extreme scenarios is related to the tail dependence at large (but finite) values. For an analysis of tail dependence of copulas see *Durante et al*. [2015], where it is also clarified how copulas sharing the same asymptotic tail dependence coefficients may differ when approaching the tail. Similar results and conclusions can be drawn considering the notion of Lower Tail Dependence [see e.g., *Salvadori et al*., 2007, sec. 3.4 and 5.3].

In general, the previous illustration is only one out of many possible counter-examples showing that it is always possible to modify the way a given probability mass is spread over the upper (or, similarly, the lower) corner of the copula domain, whatever is the dimension d—see e.g., the patchwork techniques illustrated in *Durante et al*. [2013].

4. The Failure Probability Approach

As recently discussed in *Serinaldi* [2015a], the notion of Failure Probability (hereinafter, *FP*) may provide a consistent way of assessing the hydrological (and, more generally, the environmental) risk—see also *Read and Vogel* [2015]. In this section, it is shown how Failure Probabilities can be calculated for the Hazard Scenarios investigated in this work, i.e., how to compute the probability of observing a HS at least once in a given design life time.

Let $T>0$ be an arbitrary design life time for a given structure: For the sake of simplicity, and without loss of generality, T is assumed to be measured in years. Now let $\mathbf{X}_1,\ldots,\mathbf{X}_T$ be the d-variate random vectors describing the phenomenon under investigation at times $1,\ldots,T$: for instance, think of a series of floods, modeled via the pair of annual maximum flood peak and volume. Each occurrence $\mathbf{x}_i$'s can be associated with a specific HS: for example, if $\tilde{\mathbf{x}}$ denotes a bivariate critical design threshold, then a dam might be at risk under an OR scenario when either the peak or the volume exceed the corresponding component of $\tilde{\mathbf{x}}$. In

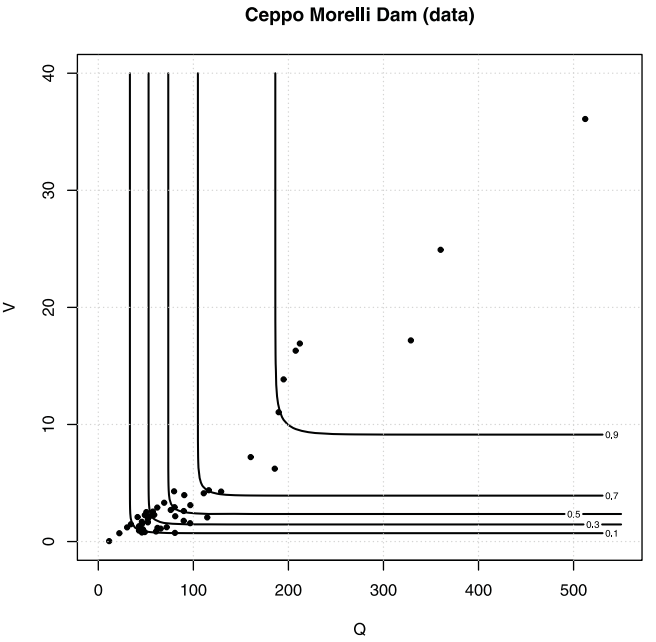

Figure 3. The available (Q, V) data—see text: the units are m^3/s for Q, and $10^6 \cdot m^3$ for V. Also shown are selected isolines of the fitted joint distribution $\mathbf{F}_{QV}$.

turn, a set of relevant Hazard Scenarios (say, $\mathcal{S}_1, \ldots, \mathcal{S}_T$) can be considered, where each HS $\mathcal{S}_i$ has a well defined level α_i: clearly, the events entailed by such HS's are dangerous ones, whereas their complements $\mathcal{S}_i^C$'s could be labeled as "safe."

Using an intuitive notation, the Failure Probability p_T can be computed as [see *Chow et al.*, 1988, chap. 12; *Kottegoda and Rosso*, 2008, chap. 9]

$$p_T = 1 - \mathbf{P}\left(\mathbf{X}_1 \in \mathcal{S}_1^C, \ldots, \mathbf{X}_T \in \mathcal{S}_T^C\right). \tag{33}$$

The formulation of equation (33) is quite a general one. For instance, if the Hazard Scenario is fixed, and the variables are i.i.d., then

$$p_T = 1 - \prod_{i=1}^{T} \mathbf{P}\left(\mathbf{X} \in \mathcal{S}^C\right) = 1 - (1-\alpha)^T. \tag{34}$$

Instead, should the Hazard Scenarios be changing in time, and the $\mathbf{X}_i$'s be independent (but, possibly, not identically distributed), then

$$p_T = 1 - \prod_{i=1}^{T} \mathbf{P}\left(\mathbf{X}_i \in \mathcal{S}_i^C\right) = 1 - \prod_{i=1}^{T} (1-\alpha_i), \tag{35}$$

where p_T is calculated by assuming that the predictive joint distribution at time i is given by a suitable function $\mathbf{F}_i$ (see Definition 2). Furthermore, should the occurrences be dependent, then an appropriate copula involving all the variables at play could be used to calculate the joint probability in equation (33)—see e.g., *Serinaldi* [2015a, equation (9)].

As an illustration, in the following the FP's corresponding to the basic HS's outlined in section 3 will be calculated for events sharing a common multivariate critical threshold $\tilde{\mathbf{x}}$, and considering independent and identically distributed $\mathbf{X}_i$'s, as is usually the case in practical applications.

1. **"OR" scenario** $\mathcal{S}^{\vee}$. According to equations (8) and (33),

$$p_T^{\vee} = 1 - \left(\mathbf{C}(F_1(\tilde{x}_1), \ldots, F_d(\tilde{x}_d))\right)^T. \tag{36}$$

2. **"AND" scenario** $\mathcal{S}^{\wedge}$. According to equations (10) and (33),

$$p_T^{\wedge} = 1 - \left(1 - \hat{\mathbf{C}}(\bar{F}_1(\tilde{x}_1), \ldots, \bar{F}_d(\tilde{x}_d))\right)^T. \tag{37}$$

3. **"Kendall" scenario** $\mathcal{S}^{\mathbf{K}}$. According to equations (12) and (33),

Table 2. Maximum Likelihood Estimates of the GEV Parameters Fitting the Variables Q and V—See Text[a]

Variable	Shape	Scale	Position	p-Value
Q (m^3/s)	0.3678	36.21	59.36	77%
	(0.11)	(5.04)	(5.71)	
V (10^6 m^3)	0.6146	1.5242	1.7229	91%
	(0.13)	(0.25)	(0.24)	

[a]The values in parentheses indicate estimated standard errors; also shown are Goodness-of-Fit test approximate p-Values (see the "R" package evir [*Pfaff et al.*, 2011].

Table 3. The Design Pairs $\tilde{\mathbf{x}}$'s—See Text[a]

	Q	V	$\alpha^{\vee}$
$\tilde{\mathbf{x}}_1$	197	14	0.0899
$\tilde{\mathbf{x}}_2$	282	17	0.0455
$\tilde{\mathbf{x}}_3$	439	31	0.0169

[a]The units are m^3/s for Q, and $10^6 \cdot m^3$ for V. Also shown are the corresponding HS levels $\alpha^{\vee}$'s.

$$p_T^{\mathbf{K}} = 1 - \mathbf{K}(t)^T, \tag{38}$$

where $t = \mathbf{F}(\tilde{\mathbf{x}})$.

4. **"Survival Kendall" scenario** $\mathcal{S}^{\check{\mathbf{K}}}$. According to equations (14) and (33),

$$p_T^{\check{\mathbf{K}}} = 1 - \check{\mathbf{K}}(t)^T, \tag{39}$$

where $t = \overline{\mathbf{F}}(\tilde{\mathbf{x}})$.

5. **"Structural" scenario** $\mathcal{S}^{\Psi}$. According to equations (16) and (33),

$$p_T^{\Psi} = 1 - \left(1 - \alpha_z^{\Psi}\right)^T, \tag{40}$$

where $z \in \mathbf{R}$ is the chosen structural threshold.

It is worth noting that, in the bivariate Extreme Value case, equation (38) has a well defined analytical expression. In fact, using equation (31), it turns out that

$$p_T^{\mathbf{K}} = 1 - (t - (1 - \tau_{\mathbf{C}})\, t \ln t)^T. \tag{41}$$

Similarly, in the bivariate Archimedean case, Theorem 4.3.4 in *Nelsen* [2006] states that $\mathbf{K}(t) = t - \gamma(t)/\gamma'(t^+)$, where γ is the (additive) inner generator of the Archimedean copula $\mathbf{C}$. In turn,

$$p_T^{\mathbf{K}} = 1 - \left(t - \gamma(t)/\gamma'(t^+)\right)^T. \tag{42}$$

For a d-dimensional generalization, Proposition 4.5 in *McNeil and Nešlehová* [2009] can be used, which provides the analytical expression of $\mathbf{K}$ for Archimedean d-copulas.

Furthermore, the switching formulas outlined in section 3.2 yield the following relations involving the Failure Probabilities associated with different bivariate scenarios:

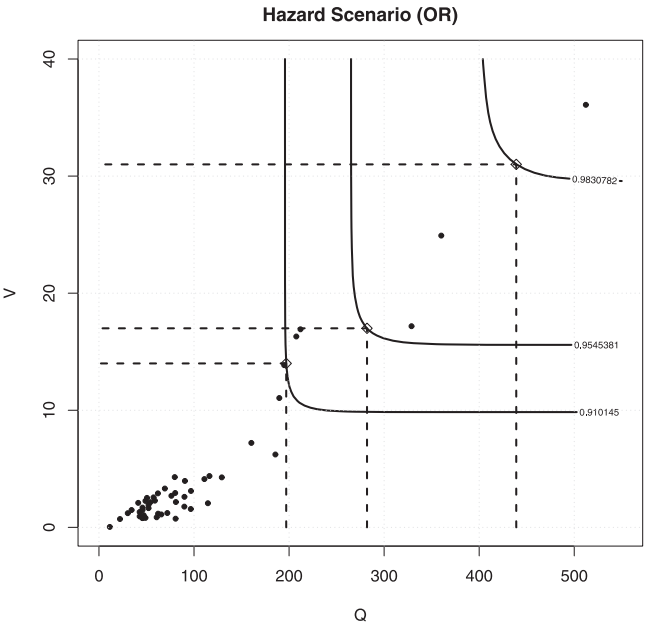

Figure 4. The available (Q, V) data (circles), and the design pairs $\tilde{\mathbf{x}}$'s (diamonds)—see text: the units are m^3/s for Q, and $10^6 \cdot m^3$ for V. The regions above and to the right of the dashed lines represent the associated OR Hazard Scenarios. Also shown are the isolines of $\mathbf{F}_{QV}$ crossing the $\tilde{\mathbf{x}}$'s, as well as the corresponding levels.

$$\begin{aligned} p_{T,\mathbf{u}}^{\vee} &= 1 - \left(-1 + u_1 + u_2 + \alpha_{\mathbf{u}}^{\wedge}\right)^T \\ &= 1 - \left(u_1 + u_2 - (1 - p_{T,\mathbf{u}}^{\wedge})^{1/T}\right)^T, \end{aligned} \tag{43}$$

$$\begin{aligned} p_{T,\mathbf{u}}^{\mathbf{K}} &= 1 - \mathbf{K}\left(-1 + u_1 + u_2 + \alpha_{\mathbf{u}}^{\wedge}\right)^T \\ &= 1 - \mathbf{K}\left(u_1 + u_2 - (1 - p_{T,\mathbf{u}}^{\wedge})^{1/T}\right)^T, \end{aligned} \tag{44}$$

and

$$\begin{aligned} p_{T,\mathbf{u}}^{\check{\mathbf{K}}} &= 1 - \check{\mathbf{K}}\left(\alpha_{\mathbf{u}}^{\wedge}\right)^T \\ &= 1 - \check{\mathbf{K}}\left(1 - (1 - p_{T,\mathbf{u}}^{\wedge})^{1/T}\right)^T. \end{aligned} \tag{45}$$

In turn, any Failure Probability can be rewritten in terms of $p_{T,\mathbf{u}}^{\wedge}$ and, conversely, $p_{T,\mathbf{u}}^{\wedge}$ can be computed as a function of the other FP's. The general case can be dealt with by using the formulas shown in Appendix A.

4.1. Multivariate Design

In order to provide valuable information for the estimate of, e.g., suitable multivariate design quantiles, further

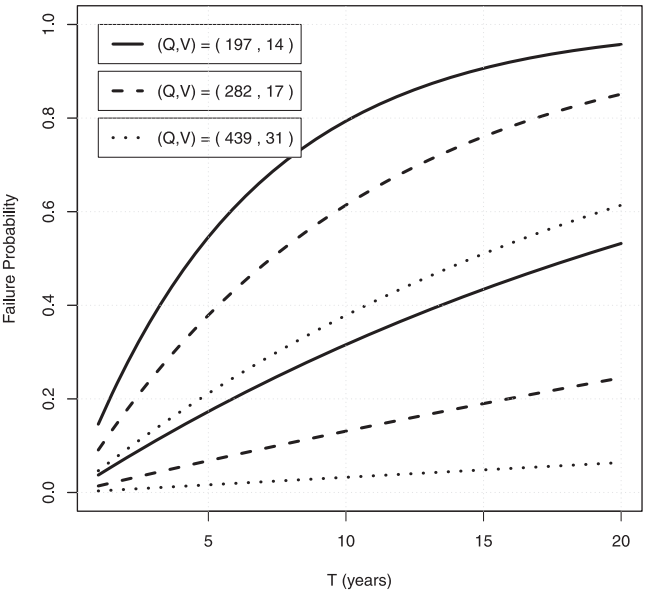

Figure 5. Confidence bands (at a 90% level) for the Failure Probabilities $p_T^{\vee}$'s associated with the design pairs $\underline{\mathbf{x}}$'s plotted in Figure 4—see text.

work may be required. In fact, considering the OR and the Kendall approaches, all the infinite realizations lying on the critical layer $\mathcal{L}_t$ are associated with the same value of the Failure Probability, since $p_T^{\vee}$ and $p_T^{\mathbf{K}}$ are constant over the level set $\mathcal{L}_t$. This may leave undetermined the assignment of a specific design occurrence, once T and p_T have been chosen (see, e.g., the illustration presented in section 5.1). The same circumstances are present in the AND and the Survival Kendall approaches, since $p_T^{\wedge}$ and $p_T^{\check{\mathbf{K}}}$ are constant over $\overline{\mathcal{L}}_t$. Instead, the Structural case requires a different approach, which will be discussed in section 5.2. In turn, valuable design values, associated with given Life Times and Failure Probabilities, could be calculated via suitable strategies, e.g., mimicking those outlined in *Chebana and Ouarda* [2011]; *Salvadori et al*. [2011]; *Corbella and Stretch* [2012]; *AghaKouchak et al*. [2014]; and *Salvadori et al*. [2014]. Practical illustrations are given below.

5. The Case Studies

In this section, two case studies are used to illustrate the practical application of the theoretical framework explained above. In section 5.1, the assessment of a dam spillway (already investigated in literature under a different theoretical framework) is reanalyzed. It is important to stress that the same procedures used in the OR case presented here can also be adopted in case other Hazard Scenarios be of interest and/or pertinent (e.g., the AND, the Kendall, or the Survival Kendall ones outlined in this work): it simply suffices to change the formulas. Thus, section 5.1 provides general how-to-do indications. In section 5.2, a structural case study concerning a preliminary design of a rubble mound breakwater (already investigated in literature under a different theoretical framework) is reanalyzed, and the calculation of Failure Probabilities and design values is illustrated.

Regarding the uncertainty analysis, in the following suitable confidence regions for the quantities of interest (viz., Failure Probabilities and design values) are calculated via a parametric bootstrap with percentile method, by generating $K = 1000$ independent random samples from the fitted model—see *Davison and Hinkley* [1997, chap. 5].

5.1. OR Example

The hydrological data investigated in the following are collected at the Ceppo Morelli dam (Northern Italy), and are the same ones investigated in *De Michele et al*. [2005] and *Salvadori et al*. [2011, 2013], to which the reader is referred. Maximum annual flood peaks Q and volumes V are identified and selected for 49 years, from 1937 to 1994 (some years are missing—see Figure 3): interestingly enough, 48 out of 49 of the occurrence dates of the Q's and the V's are the same, viz., they took place during the same flood event. Here it is assumed that the pairs are independent and identically distributed. The approach of interest is the OR one: in fact, it is sufficient that either Q, or V, or both, are large in order to affect/damage the spillway of interest.

Table 4. The Design Levels $\tilde{x}^{\vee}$'s Corresponding to Chosen Design Failure Probabilities $p_T^{\vee}$'s for the Life Time $\tilde{T} = 20$ Years—See Text[a]

$p_T^{\vee}$	$\tilde{x}^{\vee}$	Q^*	V^*
0.10	0.0053	809	90
		(338,1661)	(25,222)
0.05	0.0026	1145	156
		(393,2580)	(33,428)
0.01	0.0005	2613	569
		(546,7350)	(62,1834)

[a]Also shown are the corresponding mean "Most Likely" design pairs $\delta^* = (Q^*, V^*)$'s, as well as 90% confidence intervals (in parentheses): the units are m^3/s for Q, and $10^6 \cdot m^3$ for V.

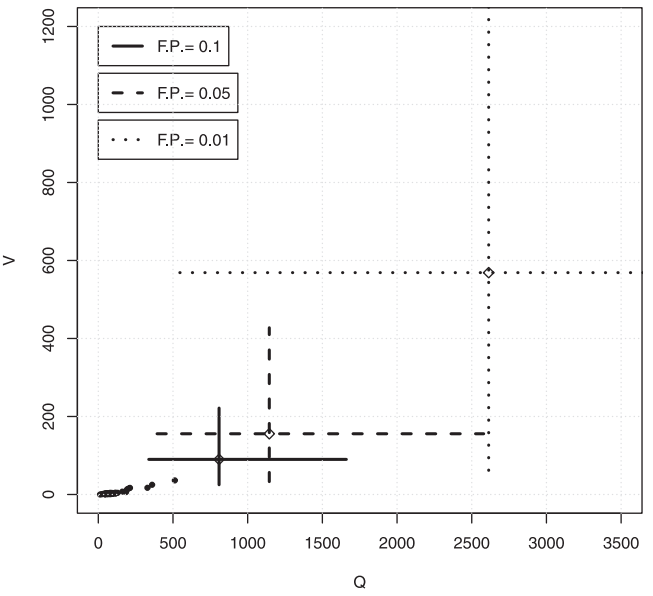

Figure 6. The available (Q, V) data (*circles*), and mean "Most Likely" design pairs $\delta^* = (Q^*, V^*)$'s (*diamonds*) for different design Failure Probabilities—see text. Also shown are confidence intervals at a 90% level.

The procedures outlined in the previous sections first require to provide a statistical framework modeling the data of interest. Here GEV marginal distributions turn out to adequately fit the observations of both Q and V (see Table 2): actually, the variables are annual maxima, and the corresponding approximate Kolmogorov-Smirnov Goodness-of-Fit test p-Values are larger than 10%. Concerning the bivariate dependence structure of the (Q, V)'s, the two variables turn out to be nonindependent. In fact, the estimates of the Kendall's $\tau_{QV} \approx 0.66$ and the Spearman's $\rho_{QV} \approx 0.80$ are both significantly positive. Here a survival-Clayton 2-copula is selected among many competing bivariate models, and provides a valuable fit of the observations: the estimate of the parameter is $\theta \approx 4.33$ (with a s.e. of about 1.38), with an approximate Cramér-von Mises Goodness-of-Fit test p-Value of about 24%. Once the margins and the copula have been fixed, the joint distribution $\mathbf{F}_{QV}$ can be computed via Sklar's Theorem: Figure 3 shows selected isolines of $\mathbf{F}_{QV}$.

For the sake of graphical illustration, a life time T, varying from one to 20 years, is chosen. Also, three design pairs $\tilde{\mathbf{x}}$'s, to be used in equations (7), (8), and (36) for the calculation of the quantities of interest, are fixed as reported in Table 3, and are plotted in Figure 4 together with the corresponding critical layers—clearly, other values could be picked out: roughly, these correspond to the empirical 90%, 95%, and 99% quantiles of, respectively, Q and V. The corresponding approximate levels $\alpha_i^\vee = 1 - \mathbf{C}_{QV}(F_Q(\tilde{x}_{i,1}), F_V(\tilde{x}_{i,2}))$, with $i = 1, 2, 3$, can be calculated via equation (8), and are reported in Table 3. As expected, (component-wise) "larger" $\tilde{\mathbf{x}}$'s yield smaller scenario levels $\alpha^\vee$'s.

Then, via equation (36), it is immediate to compute the Failure Probabilities $p_T^\vee$'s associated with the design pairs $\tilde{\mathbf{x}}$'s of interest here. The bootstrap procedure yields K independent estimates for each value of T, which can be used to evaluate the uncertainty of the $p_T^\vee$'s: as an illustration, 90% confidence bands are shown in Figure 5. Obviously, the FP's are increasingly ordered considering, respectively, the pairs $\tilde{\mathbf{x}}_3$, $\tilde{\mathbf{x}}_2$, and $\tilde{\mathbf{x}}_1$. The large variability may be explained noting that, apparently, the variance of the GEV law modeling V may not exist—see Table 2: in fact, the ML estimate of the shape parameter is larger than 1/2 (in agreement with the L-moments estimate); actually, also the shape parameter of the GEV law ruling Q is close to the critical threshold 1/2. In turn, the K samples may contain large fluctuations, which may spoil and adversely affect the calculation of the Failure Probabilities by introducing a considerable variability.

Table 5. Maximum Likelihood Estimates and Standard Errors (in Parentheses) of the Vectors of Parameters Identifying the Following Functions—See Text[a]

Variable	Shape	Scale	Position	
H (m)	1.1366	1.5235	4	
	(0.0099)	(0.0051)		
D (h)	1.1598	20.1175	0	
	(0.0077)	(0.0855)		
Variable	θ (Gumbel)	ξ (Frank)	a_1	a_2
(H, D)	2.7411	8.2117	0.5508	0.3414
	(0.2264)	(0.9788)	(0.0733)	(0.0456)

[a](Top) Generalized Weibull laws fitting the variables H and D; here the position parameters are fixed (not fitted). (*Bottom*) Bivariate "XGumbelFrank" copula fitting the pairs (H, D)'s.

Conversely, fixing T and $p_T^\vee$ (e.g., according to the recommendations given by the Regulation), it is possible to calculate a corresponding design level $\tilde{\alpha}^\vee$ by inverting equation (36):

$$\tilde{\alpha}^\vee = 1 - (1 - p_T^\vee)^{1/T}. \quad (46)$$

For the sake of illustration, here a Life Time $\tilde{T} = 20$ years is chosen, and three design values

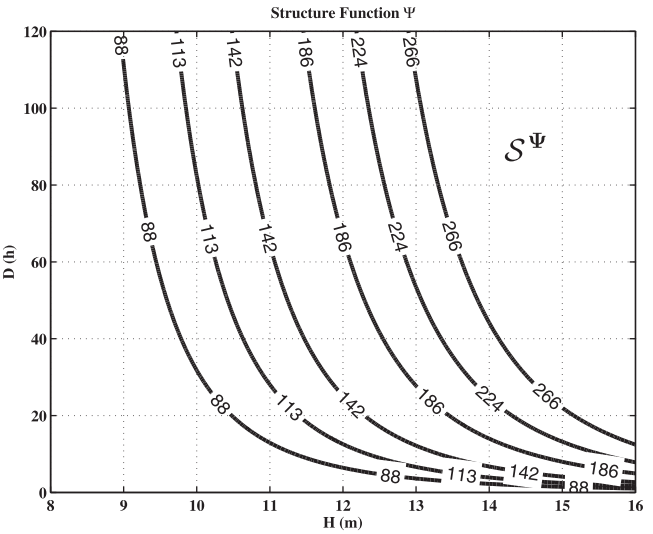

Figure 7. Selected isolines of the function $W=\Psi(H,D)$—see text: the labels indicate the design cube weights (in *tons*).

of $p\tilde{T}^{\vee}$ are selected: these are reported in Table 4, as well as the corresponding design levels $\tilde{\alpha}^{\vee}$'s.

Now the interesting point is that all the infinite OR Hazard Scenarios $\mathcal{S}^{\vee}_{\mathbf{x}}$'s, with $\mathbf{x}$ belonging to a suitable critical layer $\mathcal{L}_{\tilde{t}}$, share the same level $\tilde{\alpha}^{\vee}$, as well as the same FP $p^{\vee}_{\tilde{T}}$. In turn, bivariate design occurrences can be computed using, e.g., the strategies suggested in section 4.1. As an example, the "Most Likely" approach is used here [see *Salvadori et al*., 2011, 2014], yielding a design pair $\delta^*=(Q^*,V^*)$ given by

$$\delta^* = \underset{\mathbf{x}\in\mathcal{L}_{\tilde{t}}}{\operatorname{argmax}}\, \mathbf{f}_{QV}(\mathbf{x}), \qquad (47)$$

where $\mathbf{f}_{QV}$ is the density of $\mathbf{F}_{QV}$. Practically, δ^* simply corresponds to the pair that maximizes $\mathbf{f}_{QV}$ over $\mathcal{L}_{\tilde{t}}$: since $\mathbf{f}_{QV}$ provides a sort of (weak) likelihood for the occurrences (Q, V)'s over $\mathcal{L}_{\tilde{t}}$, the rationale is that δ^* may intuitively represent the "most likely" realization with assigned Failure Probability. The estimates of the design pairs δ^* are reported in Table 4 and plotted in Figure 6. As expected, decreasing the design FP yields (component-wise) "larger" pairs (Q^*,V^*)'s. For the same reasons discussed above, large uncertainties are present, as indicated by the bootstrap confidence intervals.

5.2. Structural Example

In order to illustrate the structural approach introduced in section 3, an example problem studied in *Salvadori et al*. [2014, 2015]—concerning a preliminary design of a rubble mound breakwater—will be reinvestigated: the target of the exercise is to compute the weight $W=\Psi(H,D)$ of a concrete unit (cube) for the case of a two-layer armored rubble mound breakwater with nonovertopping waves, where the forcing variables are the significant wave Height H (in meters), and the sea storm Duration D (in hours). For further details, the reader is referred to the two cited papers.

The available data base consists of $N=301$ bivariate sea storms (H, D)'s collected at the Alghero wave buoy (Sardinia, Italy). According to the results reported in *Salvadori et al*. [2014], the univariate margins of H and D are well fitted by Generalized Weibull laws. In addition, H and D turn out to be not independent: in fact, the estimates of the Kendall $\tau_{HD}\approx 0.54$ and the Spearman $\rho\approx 0.72$ are significantly positive. As a result, a "XGumbelFrank" 2-copula, belonging to the Khoudraji–Liebscher's family discussed in *Durante and Salvadori* [2010] and *Salvadori and De Michele* [2010] [see also *Salvadori et al*., 2014, equations (10)–(12)], turns out to provide a suitable dependence structure to model their joint random behavior. The values of the parameters used here are as reported in Table 5: in all cases (univariate and bivariate), the Goodness-of-Fit test approximate p-Values are larger than 5%.

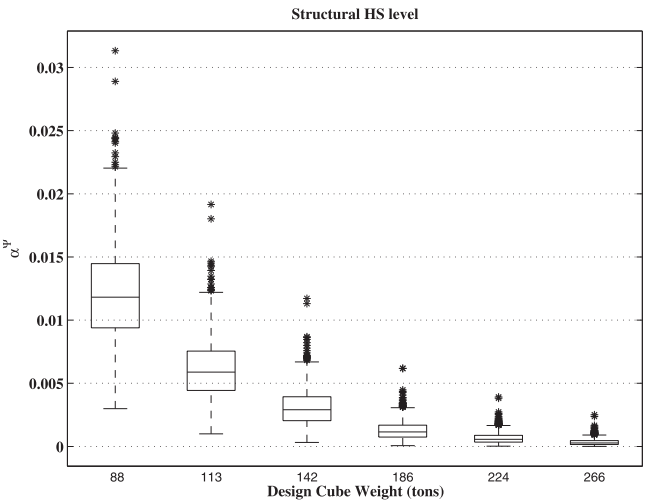

Figure 8. Estimates of the levels α^{Ψ}'s of the Structural Hazard Scenarios $\mathcal{S}^{\Psi}$'s shown in Figure 7—see text.

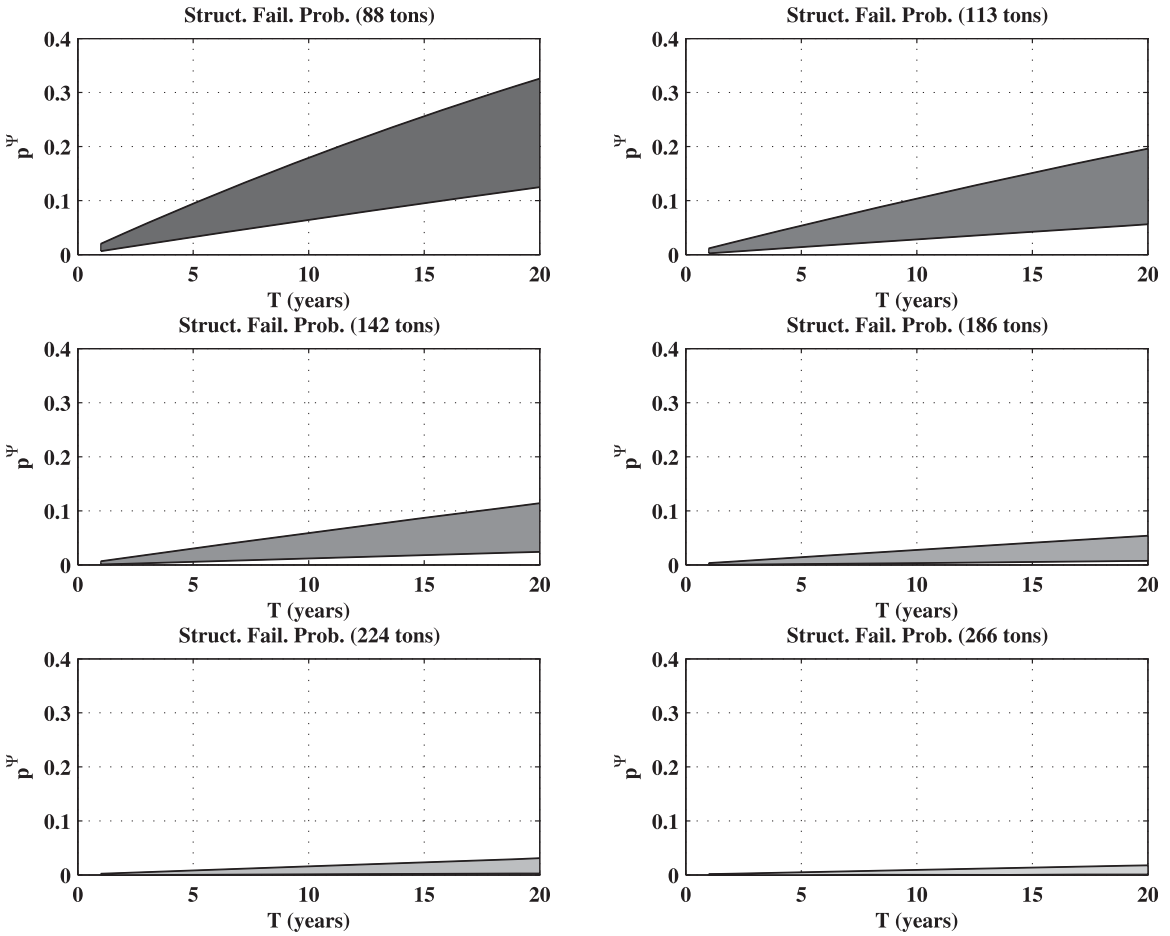

Figure 9. Confidence bands (*shaded* regions) at a 90% level of the Structural Failure Probabilities p_T^{Ψ}'s considering the design cube weights indicated in the titles—see text.

Using the Linear Wave Theory, *Goda*'s formula [*Goda*, 1974], *Van der Meer*'s [1988] formula, and the relation $T_m = 4.597 \cdot H^{0.328}$ between the average wave period T_m and the significant wave height H specifically assessed for the buoy of Alghero by *APAT* [2006, p. 29 and Table 3], the structural equation of interest here is given by

$$\begin{aligned} W &= \Psi(H, D) \\ &= \rho_S \cdot \left[H \left(\frac{2\pi H}{g\,[4.597 \cdot H^{0.328}]^2} \right)^{0.1} \right]^3 / \\ &\quad \left[\left(\frac{\rho_S}{\rho_W} - 1 \right) \cdot \left(1 + \frac{6.7 \cdot N_d^{0.4}}{(3600\, D/[4.597 \cdot H^{0.328}])^{0.3}} \right) \right]^3, \end{aligned} \tag{48}$$

where the structure function Ψ satisfies the constraints (*i*)–(*ii*) stated after equation (15), and the structural parameters g, ρ_S, ρ_W, N_d are as reported in *Salvadori et al*. [2015, Table 1].

Figure 7 shows selected isolines of the function $W = \Psi(H, D)$: here, the design cube weights are $W = 88, 113, 142, 186, 224, 266$ tons [see *Salvadori et al*., 2015, Table 2—first row]. The regions to the right of the curves represent the corresponding Structural Hazard Scenarios $\mathcal{S}^{\Psi}$'s, whose levels α^{Ψ}'s can be computed via a Monte Carlo procedure as explained below equation (16), by simulating a huge sample of size $M = 10^7$. The boxplots of the α^{Ψ}'s are obtained via 1000 bootstrap replications from the fitted model, and are shown in Figure 8: as expected, the levels decrease as the design cube weights increase.

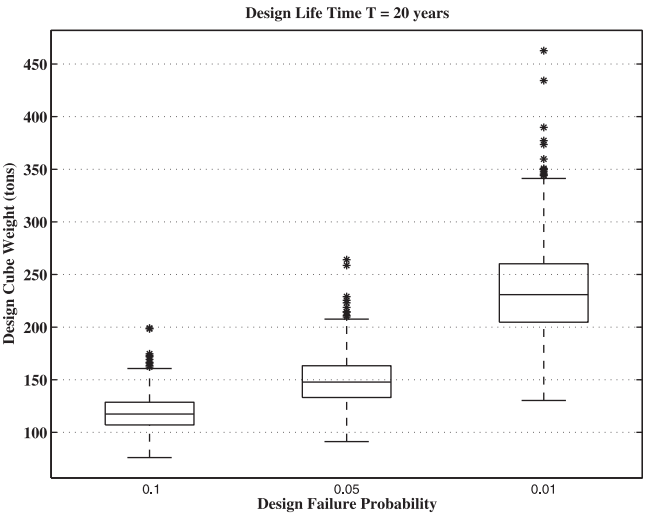

Figure 10. Estimates of the design cube weights $\tilde{W}$'s for $\tilde{T}=20$ years and given $p_{\tilde{T}}^{\Psi}$'s—see text.

The computation of the Structural Failure Probabilities p_T^{Ψ}'s is immediate via equation (40): bootstrap confidence bands are plotted in Figure 9, considering a temporal horizon of 20 years. Obviously, increasing the design cube weight reduces the corresponding Failure Probability.

Conversely, taking e.g., $\tilde{T}=20$ years as in section 5.1, and fixing $p_{\tilde{T}}^{\Psi}=10\%, 5\%, 1\%$, the corresponding design levels $\tilde{\alpha}^{\Psi}$'s can be calculated by inverting equation (40): viz., $\tilde{\alpha}^{\Psi}=1-(1-p_{\tilde{T}}^{\Psi})^{1/\tilde{T}}$. In turn, the corresponding design cube weights $\tilde{W}$ can be computed by solving equation (16) as a function of $W=z$. Again, 1000 bootstrap replications are used, and the boxplots of the results are reported in Figure 10: these provide indications about the uncertainties. As expected, the design cube weights increase for smaller and smaller Failure Probabilities.

6. Conclusions

This paper introduces a probabilistically consistent framework suitable for dealing with multivariate Hazard Scenarios, and providing valuable tools for assessing the probability of threatening of natural occurrences, according to recent EU Directives.

The concept of Hazard Scenario introduced in this work, identified via the notion of Upper Set, and characterized in terms of a specific geometry and a suitable probability level, turns out to provide a valuable tool for coherently dealing with menacing occurrences, and offers a wide variety of settings suitable for modeling various types of events. In particular, the use of Copulas gives the possibility to work out a thorough treatment of the mathematics of concern.

The Hazard Scenario framework outlined in this work well copes with the concept of Failure Probability, traditionally used in engineering practice for design and risk assessment, as well as with a Structural Approach. Furthermore, probabilities of occurrence of different HS's are calculated for the general multidimensional case ($d \geq 2$), and worthy switching formulas are presented. In addition, the Extreme Value and Archimedean special cases are dealt with, relationships between dependence ordering and scenario levels are studied, and a counter-example concerning Tail Dependence is shown.

Many practical examples are presented, and the procedures outlined in the work are illustrated via two case studies.

Appendix A: General Switching Formulas

In this Appendix, general switching formulas for the d-dimensional case, with $d>2$, are given—see section 3.2 and equation (1). The results can be obtained via recursive algorithms: in fact, the formulas for a desired $d=d^* > 2$ first require the solution of the problem for all dimensions less than d^*. Below, the set S is such that $S \subseteq \{1,\ldots,d\}$.

In the OR case,

$$\alpha^{\vee}_{u_1,\ldots,u_d}=2-\sum_{i=1}^{d} u_i+\sum_{2\leq \#(S)\leq d-1}(-1)^{\#(S)}(1-\alpha^{\vee}_S)-(-1)^d\,\alpha^{\wedge}_{u_1,\ldots,u_d}, \tag{A1}$$

where $\alpha^{\vee}_S=1-\mathbf{C}(u_j, j\in S)$ is the OR level of a HS involving only the variables whose indices are in S. Similarly, in the Kendall case,

$$\alpha^{\mathbf{K}}_{u_1,\ldots,u_d} = 1 - \mathbf{K}\left(-1 + \sum_{i=1}^{d} u_i - \sum_{2\le \#(S)\le d-1} (-1)^{\#(S)}\left(1-\alpha^{\vee}_{S}\right) + (-1)^{d}\,\alpha^{\wedge}_{u_1,\ldots,u_d}\right). \tag{A2}$$

Finally, in the Survival Kendall case,

$$\alpha^{\check{\mathbf{K}}}_{u_1,\ldots,u_d} = 1 - \check{\mathbf{K}}\left(\alpha^{\wedge}_{u_1,\ldots,u_d}\right). \tag{A3}$$

Acknowledgments

The Authors thank C. Sempi (Università del Salento, Lecce, Italy) and I. Kojadinovic (Université de Pau, Pau, France) for invaluable helpful discussions and suggestions. The data investigated in this work may be required via e-mail to the Corresponding Author. [G.S.] The support of the CMCC—Centro Euro-Mediterraneo sui Cambiamenti Climatici - Lecce (Italy) is acknowledged. [F.D.] The support of the "Faculty of Economics and Management" (Free University of Bozen-Bolzano, Italy), via the project 'FLORIDA," is acknowledged. [M.B.] The research is partially supported by the Italian Ministry of Research via the PRIN 2013–2015 ("Multivariate Statistical Methods for Risk Assessment"—MISURA), by the 2011 Sapienza University of Rome Research Project, by the "Carlo Giannini Research Fellowship," by the "Centro Interuniversitario di Econometria" (CIdE), and by the "UniCredit Foundation."

References

AghaKouchak, A. (2014), Entropy-copula in hydrology and climatology, *J. Hydrometeorol.*, *15*(6), 2176–2189, doi:10.1175/JHM-D-13-0207.1.

AghaKouchak, A., S. Sellars, and S. Sorooshian (2013), Methods of tail dependence estimation, in *Extremes in a Changing Climate, Water Science and Technology Library*, vol. 65, edited by A. AghaKouchak et al., chap. 6, pp. 163–179, Springer Sci. & Business Media, Dordrecht, Netherlands.

AghaKouchak, A., L. Cheng, O. Mazdiyasni, and A. Farahmand (2014), Global warming and changes in risk of concurrent climate extremes: Insights from the 2014 California drought, *Geophys. Res. Lett.*, *41*, 8847–8852, doi:10.1002/2014GL062308.

APAT (2006), *Atlante delle onde nei mari Italiani, Agenzia per la Protezione dell'Ambiente e per i Servizi Tecnici*, Dipartimento Tutela Acque Interne e Marine, Servizio Mareografico, Roma.

Barbe, P., C. Genest, K. Ghoudi, and B. Rémillard (1996), On Kendall's process, *J. Multivariate Anal.*, *58*(2), 197–229.

Beirlant, J., Y. Goegebeur, J. Teugels, and J. Segers (2004), *Statistics of Extremes, Wiley Ser. Probab. Stat.*, xiv+490 pp., John Wiley, Chichester, U. K.

Bender, J., T. Wahl, C. Mudersbach, and J. Jensen (2013), Flood frequency analysis and river confluences—univariate vs. multivariate extreme value statistics, in *ICWRER 2013 Proceedings*, vol. 1056, pp. 216–328.

Capéraà, P., A.-L. Fougères, and C. Genest (1997), A stochastic ordering based on a decomposition of Kendall's tau, in *Distributions With Given Marginals and Moment Problems*, edited by V. Benes and J. Stěpán, pp. 81–86, Kluwer Acad., Dordrecht, Netherlands.

Chebana, F. (2013), Multivariate analysis of hydrological variables, in *Encyclopedia of Environmetrics*, 2nd ed., edited by A. H. El-Shaarawi and W. W. Piegorsch, pp. 1676–1681, John Wiley, Chichester, U. K.

Chebana, F., and T. B. M. J. Ouarda (2011), Multivariate quantiles in hydrological frequency analysis, *Environmetrics*, *22*(1), 63–78, doi:10.1002/env.1027.

Chen, Y. D., Q. Zhang, M. Xiao, and V. P. Singh (2013), Evaluation of risk of hydrological droughts by the trivariate Plackett copula in the East River basin (China), *Nat. Hazards*, *68*(2), 529–547, doi:10.1007/s11069-013-0628-8.

Choroś, B., R. Ibragimov, and E. Permiakova (2010), Copula estimation, in *Proceedings of Copula Theory and its Applications*, *Lecture Notes Stat.*, vol. 198, edited by P. Jaworski et al., pp. 77–91, Springer, Berlin.

Chow, V. T., D. Maidment, and L. W. Mays (1988), *Applied Hydrology*, 1st ed., McGraw-Hill, Singapore.

Corbella, S., and D. D. Stretch (2012), Multivariate return periods of sea storms for coastal erosion risk assessment, *Nat. Hazards Earth Syst. Sci.*, *12*, 2699–2708, doi:10.5194/nhess-12-2699-2012.

Cousin, A., and E. Di Bernardino (2014), On multivariate extensions of conditional-tail-expectation, *Insurance Math. Econ.*, *55*, 272–282.

Davey, B., and H. A. Priestley (2002), *Introduction to Lattices and Order*, 2nd ed., Cambridge Univ. Press, Cambridge.

Davison, A. C., and D. V. Hinkley (1997), *Bootstrap Methods and Their Application, Cambridge Ser. Stat. Probabilistic Math.*, Cambridge Univ. Press, Cambridge, U. K.

De Michele, C., and G. Salvadori (2003), A Generalized Pareto intensity-duration model of storm rainfall exploiting 2-Copulas, *J. Geophys. Res.*, *108*(D2), 4067, doi:10.1029/2002JD002534.

De Michele, C., G. Salvadori, M. Canossi, A. Petaccia, and R. Rosso (2005), Bivariate statistical approach to check adequacy of dam spillway, *J. Hydrol. Eng.*, *10*(1), 50–57.

De Michele, C., G. Salvadori, R. Vezzoli, and S. Pecora (2013), Multivariate assessment of droughts: Frequency analysis and Dynamic Return Period, *Water Resour. Res.*, *49*, 6985–6994, doi:10.1002/wrcr.20551.

Dung, N. V., B. Merz, A. Bárdossy, and H. Apel (2015), Handling uncertainty in bivariate quantile estimation—An application to flood hazard analysis in the Mekong Delta, *J. Hydrol.*, *527*, 704–717, doi:10.1016/j.jhydrol.2015.05.033.

Durante, F., and G. Salvadori (2010), On the construction of multivariate extreme value models via copulas, *Environmetrics*, *21*, 143–161.

Durante, F., and C. Sempi (2015), *Principles of Copula Theory*, CRC Press, Boca Raton, Fla.

Durante, F., J. Fernández-Sánchez, and C. Sempi (2013), Multivariate patchwork copulas: A unified approach with applications to partial comonotonicity, *Insurance Math. Econ.*, *53*, 897–905.

Durante, F., J. Fernández-Sánchez, and R. Pappadà (2015), Copulas, diagonals and tail dependence, *Fuzzy Sets Syst.*, *264*, 22–41.

Embrechts, P., and M. Hofert (2013), A note on generalized inverses, *Math. Methods Oper. Res.*, *77*(3), 423–432, doi:10.1007/s00186-013-0436-7.

European Committee for Standardization (2002), *Eurocode—Basis of Structural Design*, EN 1990, European Standard.

Fan, B., L. Guo, and N. Li (2012), Copula in temporal data mining: The joint return period of extreme temperature in Beijing, in *2012 6th International Conference on New Trends on Information Science and Service Science and Data Mining (ISSDM)*, pp. 592–597.

Favre, A.-C., S. El Adlouni, L. Perreault, N. Thiémonge, and B. Bobée (2004), Multivariate hydrological frequency analysis using copulas, *Water Resour. Res.*, *40*, W01101, doi:10.1029/2003WR002456.

Fermanian, J.-D. (2013), An overview of the goodness-of-fit test problem for copulas, in *Copulae in Mathematical and Quantitative Finance, Lecture Notes Stat.*, edited by P. Jaworski, F. Durante, and W. K. Härdle, pp. 61–89, Springer, Berlin.

Ferreira, J., and C. G. Soares (2002), Modelling bivariate distributions of significant wave height and mean wave period, *Appl. Ocean Res.*, *24*(1), 31 – 45, doi:10.1016/S0141-1187(02)00006-8.

Genest, C., and A. Favre (2007), Everything you always wanted to know about copula modeling but were afraid to ask, *J. Hydrol. Eng.*, *12*(4), 347–368.

Genest, C., and L.-P. Rivest (1993), Statistical inference procedures for bivariate Archimedean copulas, *J. Am. Stat. Assoc.*, *88*(423), 1034–1043.

Genest, C., B. Rémillard, and D. Beaudoin (2009), Goodness-of-fit tests for copulas: A review and a power study, *Insurance Math. Econ.*, *44*, 199–213.

Genest, C., J. Nešlehová, and J. Ziegel (2011), Inference in multivariate Archimedean copula models, *TEST*, *20*(2), 223–256.
Ghoudi, K., A. Khoudraji, and L. Rivest (1998), Propriétés statistiques des copules de valeurs extrêmes bidimensionnelles, *Can. J. Stat.*, *26*, 187–197.
Girard, S., and G. Stupfler (2015), Extreme geometric quantiles in a multivariate regular variation framework, *Extremes*, *18*(4), 629–663, doi:10.1007/s10687-015-0226-0.
Goda, Y. (1974), New wave pressure formulae for composite breakwaters, in *Proceedings of 14th International Conference on Coastal Engineering*, pp. 1702–1720, Am. Soc. of Civ. Eng., Copenhagen.
Gräler, B. (2014), Modelling skewed spatial random fields through the spatial vine copula, *Spatial Stat.*, *10*, 87–102.
Gräler, B. (2015), *Copula Driven Spatio-Temporal Analysis, R Package Version 0.2*, 1st ed.
Gräler, B., M. J. van den Berg, S. Vandenberghe, A. Petroselli, S. Grimaldi, B. D. Baets, and N. E. C. Verhoest (2013), Multivariate return periods in hydrology: A critical and practical review focusing on synthetic design hydrograph estimation, *Hydrol. Earth Syst. Sci.*, *17*, 1281–1296, doi:10.5194/hess-17-1281-2013.
Hawkes, P. (2008), Joint probability analysis for estimation of extremes, *J. Hydraul. Res.*, *46*, suppl. 2, 246–256, doi:10.1080/00221686.2008.9521958.
Hawkes, P. J., B. P. Gouldby, J. A. Tawn, and M. W. Owend (2002), Joint probability analysis for estimation of extremes, *J. Hydraul. Res.*, *40*(3), 241–251, doi:10.1080/00221680209499940.
Hofert, M., I. Kojadinovic, M. Maechler, and J. Yan (2013), *copula: Multivariate Dependence With Copulas, R Package Version 0.999*, 7th ed.
ISO (1998), *ISO 2394—General Principles on Reliability for Structures*, Int. Organ. for Stand.
ISO (2009a), *ISO 31000—Risk Management: Principles and Guidelines*, Int. Organ. for Stand.
ISO (2009b), *ISO/IEC 31010—Risk Management: Risk Assessment Techniques*, Int. Organ. for Stand.
JCSS (2008), Risk Assessment in Engineering: Principles, System Representation & Risk Criteria, Zürich.
Jeong, D., L. Sushama, M. N. Khaliq, and R. Roy (2014), A copula-based multivariate analysis of Canadian RCM projected changes to flood characteristics for northeastern Canada, *Clim. Dyn.*, *42*(7-8), 2045–2066, doi:10.1007/s00382-013-1851-4.
Joe, H. (2014), *Dependence Modeling With Copulas*, Chapman and Hall, London, U. K.
Karmakar, S., and S. P. Simonovic (2009), Bivariate flood frequency analysis. Part 2: A copula-based approach with mixed marginal distributions, *J. Flood Risk Manage.*, *2*(1), 32–44, doi:10.1111/j.1753-318X.2009.01020.x.
Kew, S. F., F. M. Selten, G. Lenderink, and W. Hazeleger (2013), The simultaneous occurrence of surge and discharge extremes for the Rhine delta, *Nat. Hazards Earth Syst. Sci.*, *13*(8), 2017–2029, doi:10.5194/nhess-13-2017-2013.
Klein, B., A. Schumann, and M. Pahlow (2011), Copulas - New Risk Assessment Methodology for Dam Safety, in *Flood Risk Assessment and Management: How to Specify Hydrological Loads, Their Consequences and Uncertainties*, edited by A. Schumann, pp. 149–186, Springer, Dordrecht, Netherlands.
Kojadinovic, I., and J. Yan (2010), Modeling multivariate distributions with continuous margins using the copula R package, *J. Stat. Software*, *34*(9), 1–20.
Kojadinovic, I., J. Yan, and M. Holmes (2011), Fast large-sample goodness-of-fit tests for copulas, *Stat. Sin.*, *21*(2), 841–871.
Kottegoda, N., and R. Rosso (2008), *Probability, Statistics, and Reliability for Civil and Environmental Engineers*, McGraw-Hill, Oxford, Applied Statistics for Civil and Environmental Engineers, Wiley-Blackwell, Oxford.
Li, N., X. Liu, W. Xie, J. Wu, and P. Zhang (2013a), The return period analysis of natural disasters with statistical modeling of bivariate joint probability distribution, *Risk Anal.*, *33*(1), 134–145, doi:10.1111/j.1539-6924.2012.01838.x.
Li, T., S. Guo, L. Chen, and J. Guo (2013b), Bivariate flood frequency analysis with historical information based on copula, *J. Hydrol. Eng.*, *18*(8), 1018–1030, doi:10.1061/(ASCE)HE.1943-5584.0000684.
Lian, J. J., K. Xu, and C. Ma (2013), Joint impact of rainfall and tidal level on flood risk in a coastal city with a complex river network: A case study of Fuzhou City, China, *Hydrol. Earth Syst. Sci.*, *17*(2), 679–689, doi:10.5194/hess-17-679-2013.
Liu, X., N. Li, S. Yuan, N. Xu, W. Shi, and W. Chen (2015), The joint return period analysis of natural disasters based on monitoring and statistical modeling of multidimensional hazard factors, *Sci. Total Environ.*, *538*, 724–732, doi:10.1016/j.scitotenv.2015.08.093.
Masina, M., A. Lamberti, and R. Archetti (2015), Coastal flooding: A copula based approach for estimating the joint probability of water levels and waves, *Coastal Eng.*, *97*, 37–52, doi:10.1016/j.coastaleng.2014.12.010.
McNeil, A. J., and J. Nešlehová (2009), Multivariate Archimedean copulas, *d*-monotone functions and l^1-norm symmetric distributions, *Ann. Stat.*, *37*, 3059–3097.
Merz, B., H. Kreibich, and U. Lall (2013), Multi-variate flood damage assessment: A tree-based data-mining approach, *Nat. Hazards Earth Syst. Sci.*, *13*(1), 53–64, doi:10.5194/nhess-13-53-2013.
Ming, X., W. Xu, Y. Li, J. Du, B. Liu, and P. Shi (2015), Quantitative multi-hazard risk assessment with vulnerability surface and hazard joint return period, *Stochastic Environ. Res. Risk Assess.*, *29*(1), 35–44, doi:10.1007/s00477-014-0935-y.
Mitkova, V. B., and D. Halmova (2014), Joint modeling of flood peak discharges, volume and duration: A case study of the Danube River in Bratislava, *J. Hydrol. Hydromech.*, *62*(3), 186–196, doi:10.2478/johh-2014-0026.
Nappo, G., and F. Spizzichino (2009), Kendall distributions and level sets in bivariate exchangeable survival models, *Inf. Sci.*, *179*(17), 2878–2890.
Nelsen, R. (2006), *An Introduction to Copulas*, 2nd ed., Springer, N. Y.
Nelsen, R. B., J. J. Quesada-Molina, J. A. Rodríguez-Lallena, and M. Úbeda-Flores (2003), Kendall distribution functions, *Stat. Probab. Lett.*, *65*(3), 263–268.
Pfaff, B., A. McNeil, and A. Stephenson (2011), *evir: Extreme Values in R, R Package Version 1.7*, 3rd ed.
Poulin, A., D. Huard, A.-C. Favre, and S. Pugin (2007), Importance of tail dependence in bivariate frequency analysis, *J. Hydrol. Eng.*, *12*, 394–403, doi:10.1061/(ASCE)1084-0699(2007)12:4(394).
Raynal, J., and J. Salas (1987), A probabilistic model for flooding downstream of the junction of two rivers, in *Hydrologic Frequency Modeling*, edited by V. P. Singh, pp. 595–602, Springer, Netherlands.
R Core Team (2013), *R: A Language and Environment for Statistical Computing*, R Found. for Stat. Comput., Vienna.
Read, L. K., and R. M. Vogel (2015), Reliability, return periods, and risk under nonstationarity, *Water Resour. Res.*, *51*, 6381–6398, doi:10.1002/2015WR017089.
Reeve, D. (2000), *Risk and Reliability: Coastal and Hydraulic Engineering*, Spon Press, N. Y.
Reeve, D., A. Chadwick, and C. Fleming (2004), *Coastal Engineering: Processes, Theory, and Design Practice*, Spon Press, N. Y.
Requena, A. I., L. Mediero, and L. Garrote (2013), A bivariate return period based on copulas for hydrologic dam design: Accounting for reservoir routing in risk estimation, *Hydrol. Earth Syst. Sci.*, *17*(8), 3023–3038, doi:10.5194/hess-17-3023-2013.

Salas, J., and J. Obeysekera (2014), Revisiting the concepts of return period and risk for nonstationary hydrologic extreme events, *J. Hydrol. Eng.*, *19*(3), 554–568, doi:10.1061/ASCEHE.1943-5584.0000820.
Salvadori, G. (2004), Bivariate return periods via 2-copulas, *Stat. Methodol.*, *1*, 129–144.
Salvadori, G., and C. De Michele (2004), Frequency analysis via Copulas: Theoretical aspects and applications to hydrological events, *Water Resour. Res.*, *40*, W12511, doi:10.1029/2004WR003133.
Salvadori, G., and C. De Michele (2007), On the use of copulas in hydrology: Theory and practice, *J. Hydrol. Eng.*, *12*(4), 369–380, doi: 10.1061/(ASCE)1084-0699(2007)12:4(369).
Salvadori, G., and C. De Michele (2010), Multivariate multiparameter extreme value models and return periods: A copula approach, *Water Resour. Res.*, *46*, W10501, doi:10.1029/2009WR009040.
Salvadori, G., C. De Michele, N. Kottegoda, and R. Rosso (2007), *Extremes in Nature. An Approach Using Copulas, Water Science and Technology Library*, vol. 56, Springer, Dordrecht, Netherlands.
Salvadori, G., C. De Michele, and F. Durante (2011), On the return period and design in a multivariate framework, *Hydrol. Earth Syst. Sci.*, *15*, 3293—3305, doi:10.5194/hess-15-3293-2011.
Salvadori, G., F. Durante, and C. De Michele (2013), Multivariate return period calculation via survival functions, *Water Resour. Res.*, *49*, 2308–2311, doi:10.1002/wrcr.20204.
Salvadori, G., G. R. Tomasicchio, and F. D'Alessandro (2014), Practical guidelines for multivariate analysis and design in coastal and off-shore engineering, *Coastal Eng.*, *88*, 1–14, doi:10.1016/j.coastaleng.2014.01.011.
Salvadori, G., F. Durante, G. R. Tomasicchio, and F. D'Alessandro (2015), Practical guidelines for the multivariate assessment of the structural risk in coastal and off-shore engineering, *Coastal Eng.*, *95*, 77–83, doi:10.1016/j.coastaleng.2014.09.007.
Serinaldi, F. (2013), An uncertain journey around the tails of multivariate hydrological distributions, *Water Resour. Res.*, *49*, 6527–6547, doi: 10.1002/wrcr.20531.
Serinaldi, F. (2015a), Dismissing return periods!, *Stochastic Environ. Res. Risk Assess.*, *29*(4), 1179–1189, doi:10.1007/s00477-014-0916-1.
Serinaldi, F. (2015b), Can we tell more than we can know? the limits of bivariate drought analyses in the united states, *Stochastic Environ. Res. Risk Assess.*, 1–14, doi:10.1007/s00477-015-1124-3.
Shiau, J. (2003), Return period of bivariate distributed extreme hydrological events, *Stochastic Environ. Res. Risk Assess.*, *17*(1-2), 42–57.
Shiau, J. (2006), Fitting drought duration and severity with two-dimensional copulas, *Water Resour. Manage.*, *20*(5), 795–815, doi:10.1007/s11269-005-9008-9.
Shiau, J. T., and R. Modarres (2009), Copula-based drought severity-duration-frequency analysis in Iran, *Meteorol. Appl.*, *16*(4), 481–489, doi: 10.1002/met.145.
Sklar, A. (1959), Fonctions de répartition à *n* dimensions et leurs marges, *Publ. Inst. Stat. Univ. Paris*, *8*, 229–231.
Straub, D. (2014), Engineering risk assessment, in *Risk—A Multidisciplinary Introduction*, edited by C. Klüppelberg, D. Straub, and I. M. Welpe, chap. 12, pp. 333–362, Springer Int. Publ. Switzerland, N. Y., doi:10.1007/978-3-319-04486-6.
The European Parliament and The Council (2007), Directive 2007/60/EC: On the assessment and management of flood risks, *Off. J. Eur. Union*, 116 pp.
Van der Meer, J. W. (1988), Stability of Cubes, Tetrapodes and Accropode, in *Proceedings of the Breakwaters '88 Conference on Design of Breakwaters*, pp. 71–80, Inst. of Civ. Eng., London, U. K.
Volpi, E., and A. Fiori (2014), Hydraulic structures subject to bivariate hydrological loads: Return period, design, and risk assessment, *Water Resour. Res.*, *50*, 885–897, doi:10.1002/2013WR014214.
Vorogushyn, S., B. Merz, K.-E. Lindenschmidt, and H. Apel (2010), A new methodology for flood hazard assessment considering dike breaches, *Water Resour. Res.*, *46*, W08541, doi:10.1029/2009WR008475.
Wang, C., N.-B. Chang, and G.-T. Yeh (2009), Copula-based flood frequency (coff) analysis at the confluences of river systems, *Hydrol. Processes*, *23*(10), 1471–1486, doi:10.1002/hyp.7273.
Xu, K., C. Ma, J. Lian, and L. Bin (2014), Joint probability analysis of extreme precipitation and storm tide in a coastal city under changing environment, *Plos One*, *9*(10), e109341, doi:10.1371/journal.pone.0109341.
Yue, S. (2000a), Joint probability distribution of annual maximum storm peaks and amounts as represented by daily rainfalls, *Hydrol. Sci. J.*, *45*(2), 315–326, doi:10.1080/02626660009492327.
Yue, S. (2000b), The Gumbel logistic model for representing a multivariate storm event, *Adv. Water Resour.*, *24*(2), 179–185, doi:10.1016/S0309-1708(00)00039-7.
Yue, S. (2001a), A bivariate gamma distribution for use in multivariate flood frequency analysis, *Hydrol. Processes*, *15*(6), 1033–1045.
Yue, S. (2001b), A bivariate extreme value distribution applied to flood frequency analysis, *Nordic Hydrol.*, *32*(1), 49–64.
Yue, S. (2002), The bivariate lognormal distribution for describing joint statistical properties of a multivariate storm event, *Environmetrics*, *13*(8), 811–819, doi:10.1002/env.483.
Yue, S., and P. Rasmussen (2002), Bivariate frequency analysis: Discussion of some useful concepts in hydrological application, *Hydrol. Processes*, *16*, 2881–2898, doi:10.1002/hyp.1185.
Yue, S., and C. Wang (2004), A comparison of two bivariate extreme value distributions, *Stochastic Environ. Res. Risk Assess.*, *18*(2), 61–66, doi:10.1007/s00477-003-0124-x.
Zhang, L., and V. P. Singh (2012), Bivariate rainfall and runoff analysis using entropy and copula theories, *Entropy*, *14*(9), 1784–1812.
Zhang, Q., M. Xiao, V. P. Singh, and X. Chen (2013), Copula-based risk evaluation of hydrological droughts in the East River basin, China, *Stochastic Environ. Res. Risk Assess.*, *27*(6), 1397–1406, doi:10.1007/s00477-012-0675-9.